(2)

ARMY RESEARCH LABORATORY

AN ACOUSTIC SCATTERING CODE

José Lopez

Department of Electrical Engineering and Computer Science
University of Texas at El Paso
El Paso, Texas 79968

Dr. G. H. Goedecke

Department of Physics
New Mexico State University
Las Cruces, New Mexico 88003

Dr. Harry J. Auvermann

U.S. Army Research Laboratory
White Sands Missile Range, New Mexico 88002-5501

ARL-TR-53 *April 1993*

Approved for public release; distribution unlimited.

NOTICES

Disclaimers

The findings in this report are not to be construed as an official Department of the Army position, unless so designated by other authorized documents.

The citation of trade names and names of manufacturers in this report is not to be construed as official Government indorsement or approval of commercial products or services referenced herein.

Destruction Notice

When this document is no longer needed, destroy it by any method that will prevent disclosure of its contents or reconstruction of the document.

REPORT DOCUMENTATION PAGE

Form Approved
OMB No. 0704-0188

1. AGENCY USE ONLY (Leave blank)	2. REPORT DATE	3. REPORT TYPE AND DATES COVERED
	April 1993	Final

4. TITLE AND SUBTITLE
AN ACOUSTIC SCATTERING CODE

5. FUNDING NUMBERS

6. AUTHOR(S)
José Lopez, Dr. G. H. Goedecke, Dr. Harry J. Auvermann

7. PERFORMING ORGANIZATION NAME(S) AND ADDRESS(ES)
U.S. Army Research Laboratory
Battlefield Environment Directorate
ATTN: AMSRL-BE-M
White Sands Missile Range, NM 88002-5501

8. PERFORMING ORGANIZATION REPORT NUMBER
ARL-TR-53

9. SPONSORING / MONITORING AGENCY NAME(S) AND ADDRESS(ES)
U.S. Army Research Laboratory
2800 Powder Mill Road
Adelphi, MD 20783-1145

10. SPONSORING / MONITORING AGENCY REPORT NUMBER

11. SUPPLEMENTARY NOTES

12a. DISTRIBUTION / AVAILABILITY STATEMENT
Approved for public release; distribution unlimited.

12b. DISTRIBUTION CODE

13. ABSTRACT *(Maximum 200 words)*

Acoustical scattering from atmospheric turbulence is of interest to the Army because it has been identified as a candidate cause of higher than expected sound levels in shadow zones. Shadow zones are those regions where ray theory indicates no sound penetrates. Scattering into these zones may give non-line-of-sight detection through acoustic detection. This report documents the creation of a computer code for acoustic scattering from a collection of turbules or eddies. The picture is a collection of turbules of different sizes with a specified number density in each size increment. In this aspect, the picture is similar to that of optical scattering from atmospheric aerosols where there is a collection of particles of different sizes with a specified size distribution. The optical scattering code AGAUS is the starting point for creation of the Acoustic SCattering from Turbules code, ASCT, which will for acoustic scattering accomplish what AGAUS accomplishes for optical scattering. The similarities and differences between the two types of scattering are pointed out as they influence the computational algorithm.

14. SUBJECT TERMS	15. NUMBER OF PAGES
Turbules, acoustic, scattering, Mie theory	49
	16. PRICE CODE

17. SECURITY CLASSIFICATION OF REPORT	18. SECURITY CLASSIFICATION OF THIS PAGE	19. SECURITY CLASSIFICATION OF ABSTRACT	20. LIMITATION OF ABSTRACT
Unclassified	Unclassified	Unclassified	SAR

Contents

List of Figures 4

List of Tables 5

1. Introduction 7

2. Code Conversion 8

3. Cross-Section and Phase Function Results 14

4. Conclusion 15

Literature Cited 33

Appendix A. Notes on Acoustic Scattering by a Spherical Turbule 35

Appendix B. The Four Size Distribution Models of ASCT 45

Appendix C. AGAUS Formulas 47

Distribution List 49

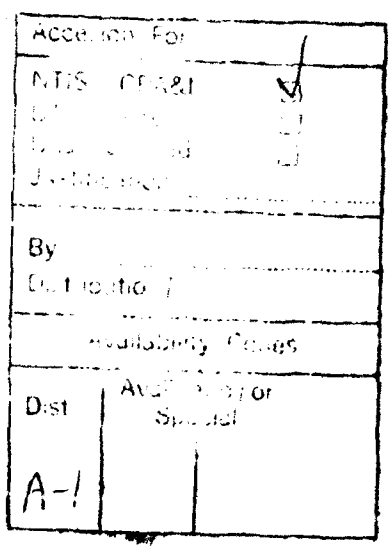

List of Figures

1. Extinction for a turbule of radius 0.5 m < r < 105 m and refractive index m = 1.0000015 17

2. Extinction for a turbule of radius 0.5 m < r < 105 m and refractive index m = 1.33333 17

3. Percent error in ASCT and ADF formula results for refractive index m = 1.0000015 18

4. Percent error in ASCT and ADF formula results for refractive index m = 1.33333 18

5. Phase function for a turbule whose radius is large compared to the wavelength 19

6. Phase function for a turbule whose radius is small compared to the wavelength 19

7. Phase function for arbitrary user-supplied model 20

8. Phase function for log-normal size distribution model 20

List of Tables

1. Table Generation Mode, m = 1.0000015 21
2. Table Generation Mode, m = 1.33333 22
3. Table Generation Mode, (Cross-Sections), m = 1.0000015 23
4. Single Turbule Model, $\lambda < r$, m = 1.0000015 24
5. Single Turbule Model, $\lambda < r$, m = 1.33333 25
6. Single Turbule Model, $\lambda > r$, m = 1.0000015 26
7. Single Turbule Model, $\lambda > r$, m = 1.33333 27
8. Arbitrary User-Supplied Model, m = 1.0000015 28
9. Arbitrary User-Supplied Model, m = 1.33333 29
10. Log-Normal Size Distribution Model, m = 1.0000015 30
11. Log-Normal Size Distribution Model, m = 1.33333 31

1. Introduction

Currently, there is great interest in acoustics within the Army because of the potential of its use for non-line-of-sight battlefield detection and location. Turbulence has been identified as a candidate cause for higher than expected sound levels within shadow zones, those regions where ray theory would indicate no sound could penetrate. Traditional turbulence theory has been developed around a model of an energy cascade through a series of eddies (hereinafter called turbules) of decreasing size until viscosity effects dissipate the energy. Traditional turbulence theory is more completely covered elsewhere (Noble and Auvermann, 1993). The theory goes immediately into statistical averages with no further interest in the internal structure of the turbulent region. This traditional theory is therefore termed the "statistical approach" to turbulence. More recently as experimental evidence has accumulated, interest has developed in the "structural approach" to turbulence wherein the effect of internal structure is more adequately accounted for. There is a natural parallel between optical scattering from aerosols and acoustical scattering from turbules. This parallel comes from the similarity between the picture of atmospheric aerosols as a collection of spherical particles of varying index-of-refraction and size and the picture of a turbulent region as a collection of spherical eddies with varying wave speeds and sizes. To determine scattering from such collections, the scattering from each size of scatterer must be determined and then the sum from some specified size distribution calculated. This is exactly the function of the optical scattering code AGAUS.

Program AGAUS was developed several years ago to determine electromagnetic scattering properties of small spherical particles. This report is concerned with the conversion of the AGAUS code from an optical scattering code to an acoustical scattering code. The notion is that the temperature distribution within a turbule creates an accompanying sound speed distribution that will cause the sound speed within the turbule to be different from that outside the turbule. There is thus an acoustic index of refraction discontinuity caused by the turbule in the same way an aerosol particle causes an optical index of refraction discontinuity. Acoustical scattering is also caused by the velocity distribution. This is not treated here. The index of refraction variation within a turbule is treated as an average quantity so it is uniform within the spherical volume occupied by the turbule. One other difference between optical scattering and acoustic scattering is that the index variations in turbulence are very slight as compared to index variations in aerosols distributions. One should be careful to calculate with sufficient precision so that the effects are not lost in computer round off errors. Small temperature variations between the inside and outside of a turbule result in refractive indices near 1. Hence, the conversion of program AGAUS from single precision to quadruple precision was accomplished, resulting in the code called QGAUS. This conversion is described elsewhere (Nguyen, 1993). The conversion to acoustic scattering began with QGAUS.

Electromagnetic scattering code AGAUS utilizes Mie theory for determining the scattering properties of spherical homogeneous particles. Mie theory predicts the scattering and absorption of electromagnetic radiation of wavelength λ by spherical particles of radius r having refractive index $m = n + ik$ relative to the propagation

medium. A complex refractive index is used in the optical code AGAUS to account for a lossy propagation medium, and this usage is retained in the acoustic scattering code ASCT. Program runs of ASCT were performed with the imaginary component of the complex refractive index m set to zero as only real refractive indices were of interest. Particles in space attenuate incident electromagnetic radiation by scattering the radiation in different directions and absorption within the particle. Extinction is the sum of the scattering and the absorption. Extinction, scattering, and absorption of a particle are characterized by effective "blocking" areas or cross-sections (C_{ext}, C_{sca}, C_{abs}). The angular distribution of the scattered radiation of spherical particles is characterized by the phase function $p(\theta)$, a function of the single variable θ that is the angle between the direction of propagation and the direction to the observation position. The cross-sections and phase function are dependent on the particles' refractive index and size parameter $x = 2\pi r/\lambda$, where r is the particle radius and λ is the radiation wavelength. Mie theory provides a method for calculating the cross-sections and phase function as a series expansion of the field into partial waves (monopole, dipole, quadrapole, etc). A detailed description of the theory can be found in Bohren (1983).

Because electromagnetic and acoustic wave propagation both obey the wave equation, the same theory can be used to determine acoustic scattering properties of spherical turbules. For electromagnetic waves Mie theory matches partial wave expansion coefficients at the particle boundary so that both the electric field (E) and the magnetic field (H) are solutions of the wave equation inside and outside the particle. When Mie theory is applied to acoustic waves, the solution to the wave equation involves matching partial wave expansion coefficients for the sound wave pressure and velocity at the turbule boundary. A detailed derivation of expansion coefficients expressions for acoustical scattering by a uniform density spherical turbule has been provided through a separate contract (appendix A). Analytical formulae from this derivation were used in the conversion of QGAUS to the acoustic scattering code.

Details of the conversion of electromagnetic scattering code QGAUS to acoustic-scattering code ASCT (for Acoustical SCattering from Turbules) are presented in section 2. Representative results for the cross-sections and phase function are presented in tables and graphs in section 3. Code verification is obtained by a comparison of code results for extinction with approximate analytical formula results. Conclusions concerning the conversion and results are presented in section 4. Appendix B describes the four size distributions that may be chosen in ASCT. The electromagnetic scattering formulas that are the basis of AGAUS are included in appendix C to compare with the corresponding acoustic formulas more easily.

2. Code Conversion

A detailed description of AGAUS can be found in Miller (1983). Since Program QGAUS is identical to Program AGAUS except that all calculations are done in quadruple precision, the description in Miller (1983) is directly applicable to QGAUS. All work described in this report and in Nguyen (1993) was done on a Hewlett-Packard 9000/780 mainframe using HP FORTRAN 77/HP-UX. The only significant

computational differences between AGAUS and QGAUS result from the absence of quad precision complex arithmetic operations. Appropriate quad precision real operations were substituted where necessary and combined to give a quad precision complex result. Program QGAUS has 10 modes of operation defined by 10 different particle size distribution models. Inputs to QGAUS include wavelength, complex refractive index, and 11 integer program control parameters. Program output consists of cross-sections and phase function tables. Mie calculations are performed in subroutine MIEGX. Variable parameters to subroutine MIEGX include the size parameter $x = 2\pi a/\lambda$ and the refractive index $n = m + ik$. MIEGX returns scattering efficiency factors from which the scattering cross-sections and phase function are calculated.

Conversion of program QGAUS to an acoustic scattering code involved redefinition of the formulas used in subroutine MIEGX for determining the efficiency factors. Subroutines AGAUG and WATER were deleted since the new code will not be used to treat hygroscopic effects. Control parameter IW was redefined as ICQ and is used for printing either efficiency factors (ICQ = 0) or cross-sections (ICQ = 1). Program QGAUS used units of micrometers for wavelength and particle radius and square centimeters for the cross-sections. The modified code uses units of meters for the wavelength and turbule radius and square meters for the cross-sections. Six of the 10 distribution models were deleted since they had no bearing on the problem of acoustic scattering by spherical turbules. A description of the four remaining models, as well as the inputs required by each, is given in appendix B.

Subroutine MIEGX has been modified to compute scattering properties of spherical turbules via the expansion coefficient a_ℓ, which corresponds to the induced electric multipole moment in electromagnetic scattering problems. The expansion coefficient a_ℓ is defined as follows:

$$-a_\ell = \frac{mj_\ell'(mx)j_\ell(x) - j_\ell(mx)j_\ell'(x)}{mj_\ell'(mx)h_\ell^{(1)}(x) - j_\ell(mx)h_\ell^{(1)\prime}(x)}, \tag{1}$$

where $j_\ell(z)$ and $h_\ell(z)$ are the spherical Bessel function and the Hankel function of the third kind, respectively. The prime means "derivative with respect to the argument." For computational purposes a_ℓ is rewritten as

$$-a_\ell = \frac{[mA_\ell(mx) + \frac{\ell+1}{x}]\mathrm{Re}[\xi_\ell(x)] - \mathrm{Re}[\xi_{\ell-1}(x)]}{[mA_\ell(mx) + \frac{\ell+1}{x}]\xi_\ell(x) - \xi_{\ell-1}(x)}, \tag{2}$$

where

$$A_\ell(mx) = \frac{j'_\ell(mx)}{j_\ell(mx)} = \frac{j_{\ell-1}(mx)}{j_\ell(mx)} - \frac{(\ell+1)}{mx}$$
$$= -\frac{\ell}{mx} + \frac{j_{\ell-1}(mx)}{j_\ell(mx)} - \frac{1}{mx}, \tag{3}$$

and $\xi(x)$ is the Ricatti-Bessel function of the third kind and is related to the Bessel function $j_\ell(z)$ by

$$\xi_\ell(z) = zj_\ell(z) - izy_\ell(z). \tag{4}$$

The difference of the first two terms of the quantity $A_\ell(mx)$ is computed using Lentz's continued fraction method. Detailed information on this method can be found in Lentz (1976).

The cross-sections, scattering amplitude, differential scattering amplitude, and phase function are defined as follows:

The extinction cross-section is given by

$$\sigma_{ext}(k) = \frac{-4\pi}{k^2}\sum_{\ell=0}^{\infty}(2\ell+1)\Re e(a_\ell), \tag{5}$$

the scattering cross-section is given by

$$\sigma_{sca}(k) = \frac{4\pi}{k^2}\sum_{\ell=0}^{\infty}(2\ell+1)|\,a_\ell|^2, \tag{6}$$

the absorption cross-section is given by

$$\sigma_{abs}(k) = \sigma_{ext}(k) - \sigma_{sca}(k), \tag{7}$$

the radar cross-section is given by

$$\sigma_{rad}(k) = \frac{4\pi}{k^2} \left| \sum_{\ell=0}^{\infty} (2\ell+1)(-1)^{\ell} a_{\ell} \right|^2, \tag{8}$$

the scattering amplitude is given by

$$f(k,\theta) = \frac{1}{ik} \sum_{\ell=0}^{\infty} (2\ell+1) a_{\ell} P_{\ell}(\cos\theta), \tag{9}$$

where $P_\ell(\cos\theta)$ is the Legendre polynomial function and is computed in MIEGX using the following recurrence formula

$$(2\ell+1)xP_\ell(x) = (\ell+1)P_{\ell+1}(x) + \ell P_{\ell-1}(x),$$

the differential scattering cross-section is given by

$$\sigma(k,\theta) = |f(k,\theta)|^2, \tag{10}$$

and the phase function is given by

$$p(\theta) = \frac{|f(k,\theta)|^2}{k^2 \sigma_{sca}(k)}, \tag{11}$$

for $k = 2\pi/\lambda$.

The radar cross-section and phase function were defined according to those given in Bohren (1983). Subroutine MIEGX computes efficiency factors Q_{ext}, Q_{sca}, Q_{abs}, and Q_{rad}, from which the cross-sections are computed. The efficiency factors are multiplied by the geometrical sphere cross-section to obtain the true cross-sections $C_i = \pi r^2 Q_i$ in the main program.

The efficiency factors are defined as follows:

$$Q_{ext} = -\frac{4}{x^2} \sum_{\ell=0}^{\infty} (2\ell+1) \Re e(a_\ell), \tag{12}$$

$$Q_{sca} = \frac{4}{x^2}\sum_{l=0}^{\infty}(2l+1)|\,a_l|^2, \tag{13}$$

$$Q_{ext} = \frac{4}{x^2}\left|\sum_{l=0}^{\infty}(2l+1)a_l(-1)^l\right|^2. \tag{14}$$

As mentioned above the difference of the first two terms of the quantity $A_\ell(mx)$ is computed via the continued fraction method (Lentz, 1976). This method is valid for ℓ = 1,2,3,...etc. Equations (5) through (14) require computation of $A_\ell(mx)$ for $\ell = 0$, which is not possible with the continued fraction method. Subroutine A0 was developed to handle computation of $A_\ell(mx)$ for $\ell = 0$. A_0 is defined as follows:

$$A_0(mx) = \frac{j_{-1}(mx)}{j_0(mx)} - \frac{1}{mx}, \tag{15}$$

where

$$j_{-1}(mx) = \frac{\cos(mx)}{mx},$$
$$j_0(mx) = \frac{\sin(mx)}{mx}. \tag{16}$$

Substituting equation (16) into equation (15) yields,

$$A_0(mx) = \frac{\cos(mx)}{\sin(mx)} - \frac{1}{mx}. \tag{17}$$

The argument mx may be complex. Hence, computing of the ratio cos(mx)/sin(mx) is done in subroutine A0 by defining cos(mx) and sin(mx) as follows:

$$\cos(mx) = \frac{e^{imx} + e^{-imx}}{2},$$
$$\sin(mx) = \frac{e^{imx} + e^{-imx}}{2i}. \tag{18}$$

Once the quantity $A_\ell(mx)$ is computed for $\ell = 0$, the remaining terms (for $\ell =$ 1,2,3...etc) are computed via the continued fractions method already coded in subroutine MIEGX.

For small size parameter x, the dominant term in the summations of equations (5) through (14) is a_0. Subroutine MIEGX bypasses the continued fraction calculations in this case, calls subroutine A0, and computes the efficiency factors and phase function using only the term a_0.

A comparison of the formulas implemented in program AGAUS to those implemented in the acoustic code reveals both similarities and differences between the two sets of formulas. Appendix C contains the definitions of the formulas implemented in program AGAUS. The corresponding formulas implemented in the acoustic code are given by equations (2), (3), (12), (13), (14), and (11).

A comparison of equation (2) with equations (C-1) and (C-2) shows that the formula for the expansion coefficient a_ℓ given by equation (2) is most like the formula for the expansion coefficient b_ℓ given by equation (C-2). Equation (2) and (C-2) differ in the term $(\ell+c)/x$ where $c = 0$ in equation (C-2) and $c = 1$ in equation (2). Another difference between equation (2) and (C-2) is in the definition of the term $A_\ell(mx)$. Equations (3) and (C-3) give, respectively, the acoustic and electromagnetic code formulas for the term $A_\ell(mx)$. The two formulas are the same except for the absence of the term -1/mx in equation (C-3). The formulas for the extinction, scattering, and radar efficiency factors for the acoustic and electromagnetic codes are given in equations (12) through (14), and equations (C4) through (C6), respectively. The formulas given by equations (C-4) through (C-6) are dependent on both expansion coefficients a_ℓ and b_ℓ whereas those given by equations (12) through (14) are dependent only on the expansion coefficient a_ℓ. Also, the summation coefficient $4/x^2$ shown in equations (12) and (13) is twice the coefficient $2/x^2$ shown in equations (C-4) and (C-5), and four times the coefficient shown in equation (C-6).

The formulas for the phase function are given by equations (11) and (C-13). Computation of the phase function in program AGAUS is also dependent on the expansion coefficients a_ℓ and b_ℓ and the angular factors $\pi_\ell(\theta)$ and $\tau_\ell(\theta)$. In contrast, the phase function given by equation (11) is dependent on the expansion coefficient a_ℓ and the Legendre polynomial function $P_\ell(\cos\theta)$. Furthermore, the coefficient $1/2k^2$ shown in equation (C-13) is half of the coefficient shown in equation (11). Finally, the summations computed in program AGAUS (see equations (C-4) through (C-8) begin with $\ell = 1$, whereas the summations computed in the acoustic code (see equations (9), and (12) through (14)) begin with $\ell = 0$. Appropriate changes were made to the formulas implemented in program QGAUS based on the differences mentioned above to convert it to acoustic scattering code ASCT.

Program ASCT operates under four distinct modes. In type 0 mode the user enters a set of radii and corresponding absolute number densities. The program calculates the cross-sections and phase function for each radii and sums the contribution of each to get the

total cross-sections and phase function. In type 1 mode a log-normal distribution function is used to determine the radii at which the cross-sections and phase function are calculated. In type 2 mode cross-section and phase function are calculated for a single turbule radius. In type 3 mode a table of cross-sections (ICQ = 1) or efficiency factors (ICQ = 0) versus turbule radius is generated. Appendix B describes the four modes as well as program input requirements. The code verification method and the results obtained are discussed in section 3.

3. Cross-Section and Phase Function Results

The code was verified by comparing the values for extinction efficiency obtained from program ASCT to those obtained from "anomalous diffraction" formula (ADF) given below,

$$Q_{ext} = 2 - \frac{4}{\rho}\sin\rho + \frac{4}{\rho^2}(1 - \cos\rho), \tag{19}$$

where $\rho = 2x|m-1|$. Equation (19) was derived in Van de Hulst (1957) and is good for large size parameter x (that is, for $\lambda \ll r$) and refractive indices near 1 (that is, $m = 1 \pm \epsilon$). For small size parameter x (that is, $\lambda \gg r$), the following equation was derived for comparison,

$$Q_{ext} = \frac{4}{9}x^4|m^2 - 1|^2. \tag{20}$$

Equation (20) was derived following the method used in Bohren (1983) for particles small compared to the wavelength. See also reference Morse (1968), page 427.

Program ASCT and ADF results for extinction efficiency are shown in figures 1 and 2, for refractive indices m = 1.0000015 and m = 1.33333, respectively. The authors recognized that 1.33333 is far too large to represent an acoustic index of refraction. This index is used here solely as a means to exercise and check the code in the large size parameter regime. To get results where Q_{ext} flattens out for an index of 1.02 would require an enormous size parameter, for which the run time would have been prohibitive. Figure 1 gives the extinction curve for a turbule of radius 0.5 m < r < 105 m, wavelength λ = 5 m, and refractive index m = 1.0000015. The corresponding data for figure 1 is shown in table 1. Program ASCT extinction efficiency values are given in column Q(EXT), and the extinction predicted by ADF is given in the column so marked.

Figure 2 shows the extinction efficiency curve for a turbule having refractive index m = 1.33333 and radius 0.5 m < r < 105 m. Table 2 shows the corresponding data for

figure 2. For refractive index m = 1.0000015, the average percent error between the program and formula extinction efficiencies is ≈ 0.04 percent; and for refractive index m = 1.33333, the average percent error is ≈ 7.4 percent.

Figures 3 and 4 are plots of the percent error versus size parameter x for refractive indices m = 1.0000015 and m = 1.33333, respectively. Table 3 simply shows cross-sections rather than efficiency factors for turbule radius 0.5 m < r < 45 m, wavelength λ = 15 m, and refractive index m = 1.0000015. The ADF formula was derived assuming a refractive index near 1 and a large size parameter x (that is, r ➤ λ). Table 1 and figure 3 show clearly good agreement between program ASCT and formula results for refractive index m = 1.0000015. For refractive index m = 1.33333, program ASCT and formula results differ slightly. This should be expected since the refractive index is greater than 1.

Figure 4 shows an improvement in the error for increasing size parameter x. This is in accordance with the large size parameter assumption of the formula. Using the parameters of table 1 for radius of 0.5 m, equation (20) gives an extinction efficiency of 6.234E-13, which is only 14.4 percent different than the program results. Using the parameters of table 1 for a radius of 0.05 m, equation (20) gives an efficiency of 3.23320E-09 and the ASCT program gives a result of 3.23328E-09, indicating the improved agreement for smaller size parameter. In this latter case, the angular dependence of the scattering is very nearly isotropic, which is consistent with the fact that monopole is the dominant mode of scatter when x is small.

The phase function gives out information about the angular distribution of the scattered wave. Figure 5 shows the phase function curve for a turbule whose radius (r = 30 m) is large compared to the wavelength (λ = 5 m) for refractive indices m = 1.0000015 and m = 1.33333. Figure 6 shows the phase function curve for a turbule whose radius (r = 5 m) is small compared to the wavelength (λ = 30 m). Figure 7 shows the phase function for a user-supplied distribution of turbule radii. The phase function for a log-normal distribution of turbule radii is shown in figure 8. Tables 4 through 11 show the corresponding data for figures 5 through 8. The results obtained from program ASCT are in accord with those predicted by the "anomalous diffraction" formula and the small size approximation. ASCT correctly models the acoustic scattering properties of spherical turbules.

4. Conclusion

An acoustic scattering code, Program ASCT, is now available for determining the scattering properties of nonrotational spherical turbules. It can generate the cross-sections and phase function for four modes of operation. Program ASCT was developed by inserting acoustic interface relations in the electromagnetic scattering QGAUS code. QGAUS was, in turn, developed from the AGAUS code through conversion to quadruple precision arithmetic. The majority of the modifications to program QGAUS were in subroutine MIEGX, where the main Mie calculations are performed. Modifications to this routine were based on the derivations provided by Dr. G. H. Goedecke. These

derivations were compared to cross-section and phase function equations given in Morse (1968) for scattering by spherical particles. Aside from different notation used, the formulas for the cross-sections and phase function were found to be identical. The extinction results from program ASCT were then compared to those predicted by the "anomalous diffraction" formula and found to be in remarkably good accord. Thus, there is now available an accurate code for determining the acoustic scattering properties of spherical turbules modeled as uniform acoustic index-of-refraction inhomogeneities. The angular dependenee for small size parameter was compared to that found in Morse (1968, page 427). Morse shows an angular dependence with predominant scattering in the backward direction. ASCT results show an isotropic scattering pattern. The difference is caused by the different boundary conditions for the two derivations. Morse considers a scatterer with a definite surface. For this case, the boundary conditions are that pressure is continuous and that the normal velocity is continuous. ASCT considers a scatterer without a definite surface. In the ASCT case, the boundary conditions are that the pressure is continuous and that the mass flow (density times velocity) is continuous. Morse shows the dipole term contributes to the lowest order of scattering. In ASCT, only the monopole term contributes to the lowest order of scattering.

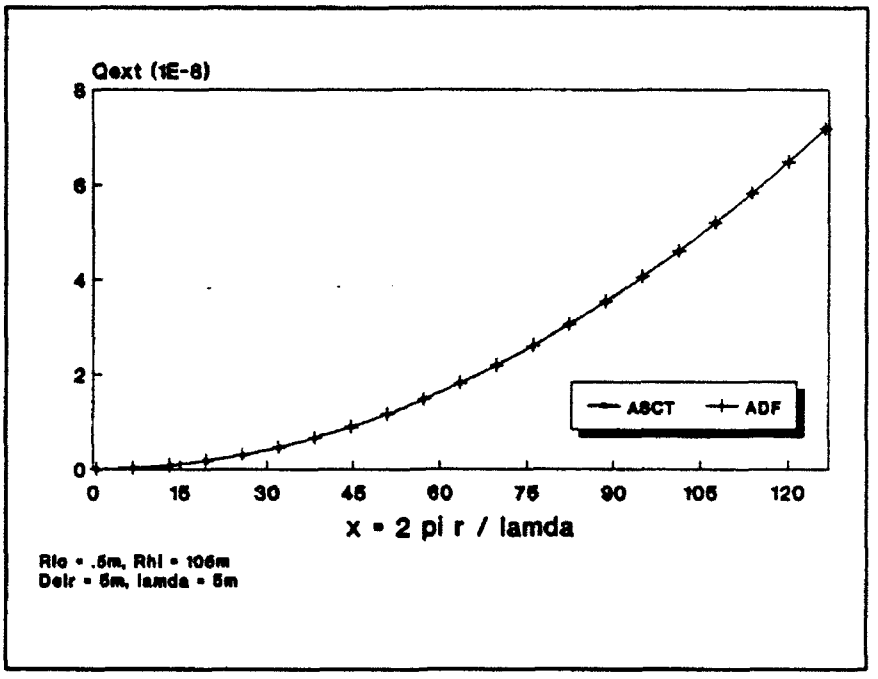

Figure 1. Extinction for a turbule of radius 0.5 m < r < 105 m and refractive index m = 1.0000015.

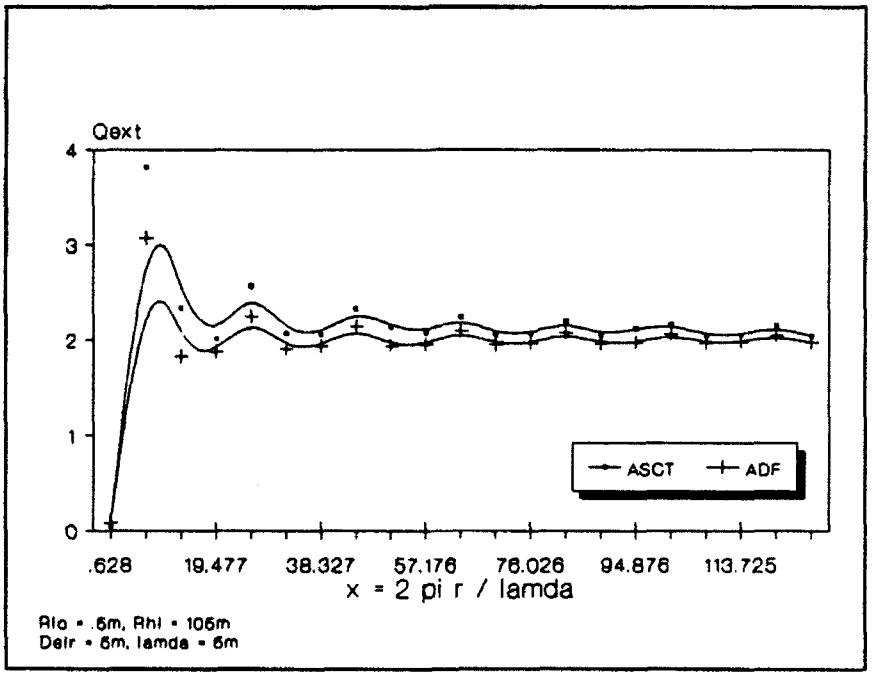

Figure 2. Extinction for a turbule of radius 0.5 m < r < 105 m and refractive index m = 1.33333.

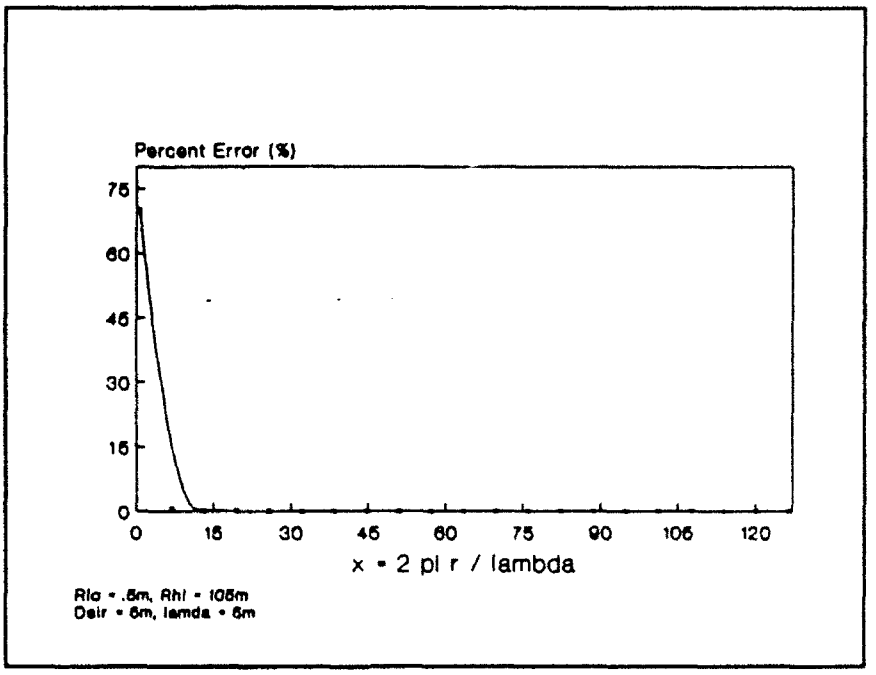

Figure 3. Percent error in ASCT and ADF formula results for refractive index m = 1.0000015.

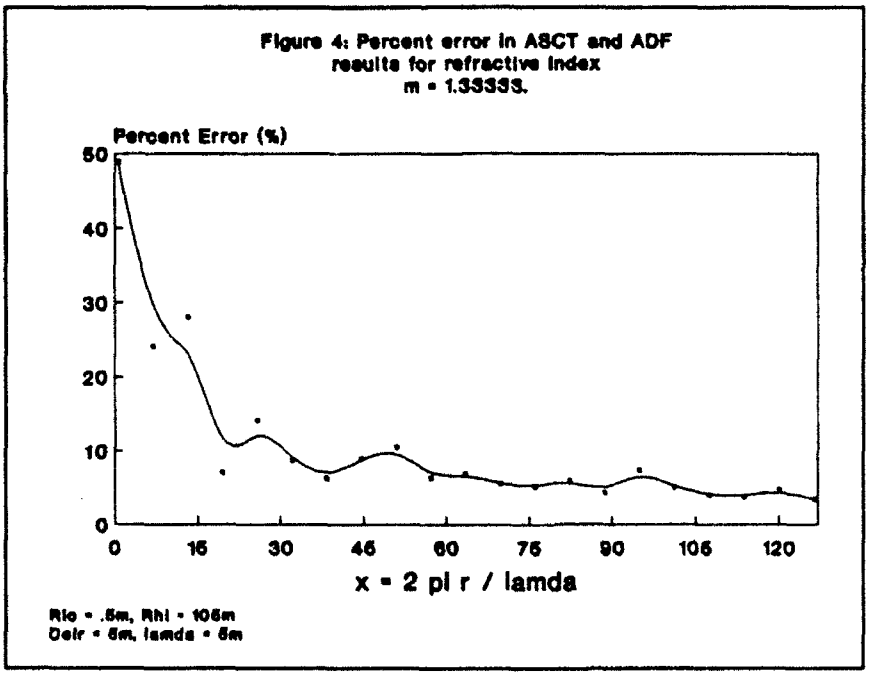

Figure 4. Percent error in ASCT and ADF formula results for refractive index m = 1.33333.

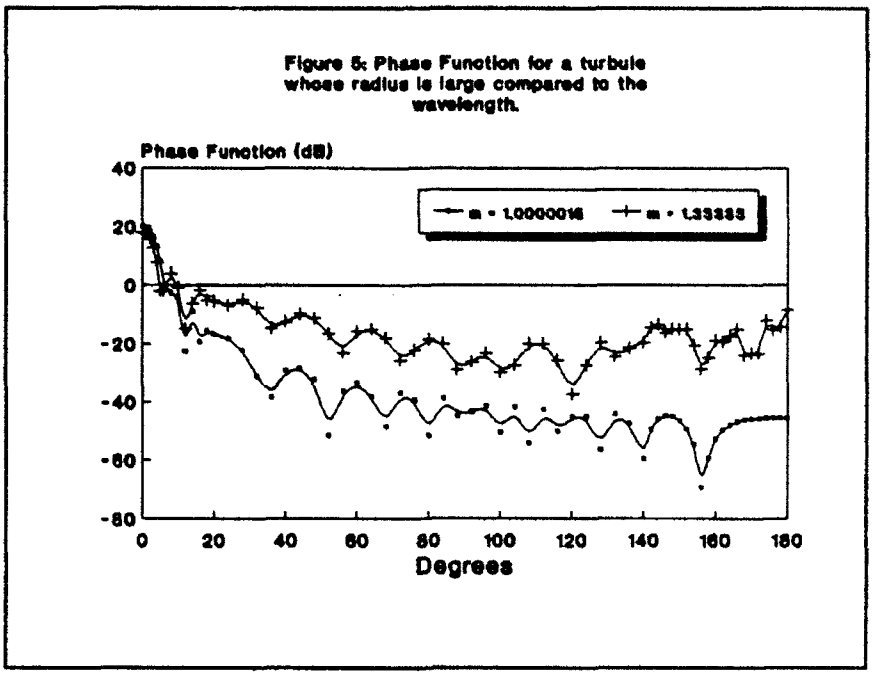

Figure 5. Phase function for a turbule whose radius is small compared to wavelength.

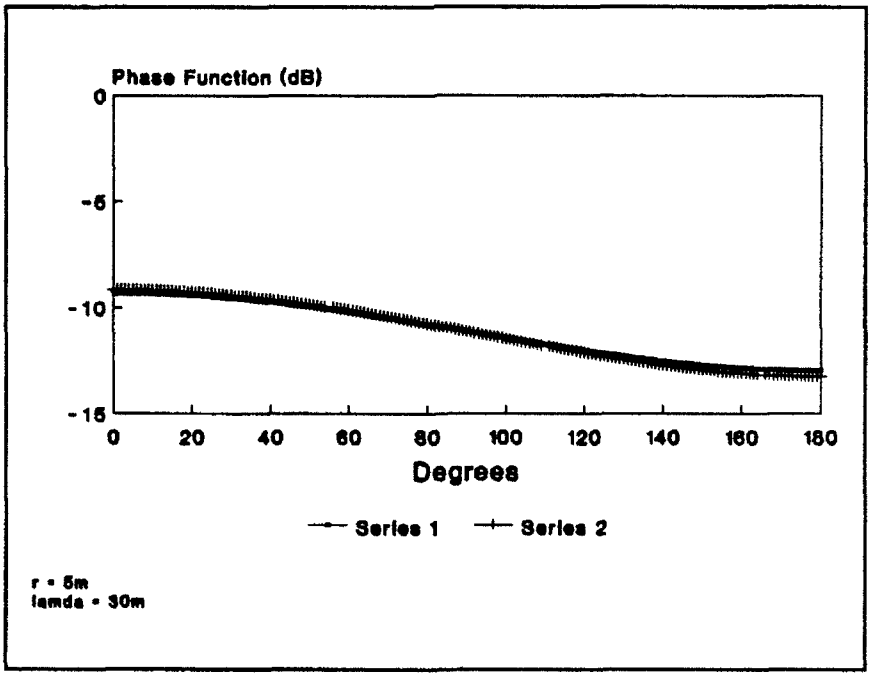

Figure 6. Phase function for a turbule whose radius is small compared to wavelength.

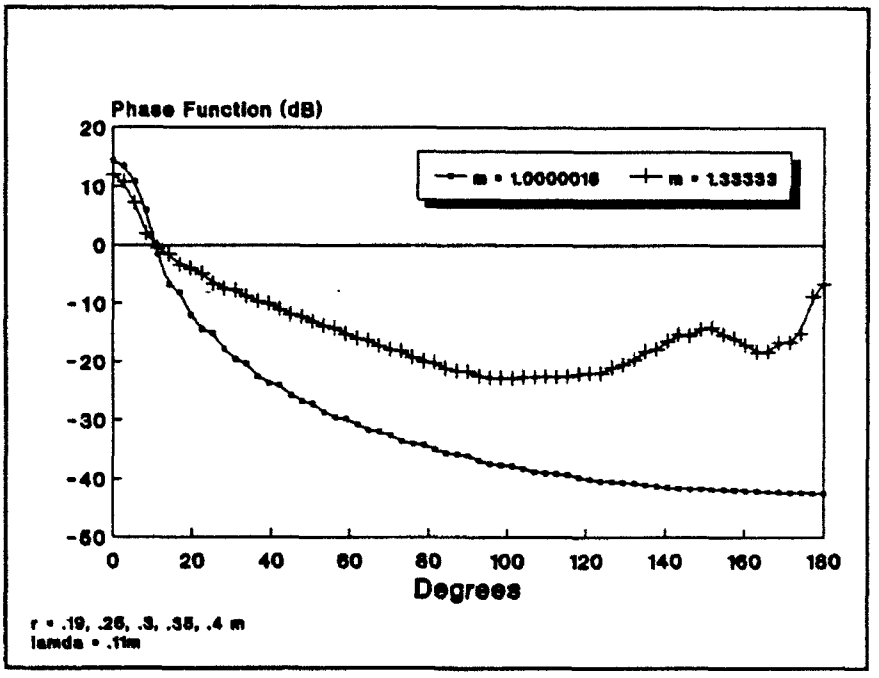

Figure 7. Phase function for arbitray user-supplied model.

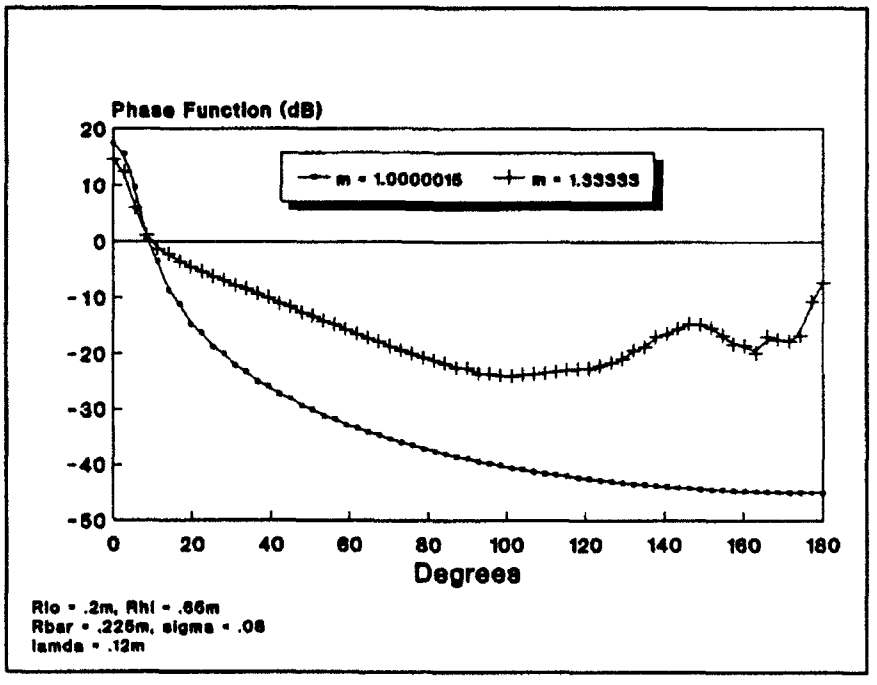

Figure 8. Phase function for log-normal size distribution model.

TABLE 1. TABLE GENERATION MODE

m = 1.0000015

RLO = 5.00000E-01. RHI = 1.05000E+02. DELR = 5.00000E+00
Wavelength = 5.00 m
Real Index = 1.00000150 Imag. Index = .00000000

R(m)	Size Parameter	Q(EXT)	Q(SCA)	Q(ABS)	ADF
.50000	6.28319E-01	5.33358E-13	5.33358E-13	0.00000E+00	1.77653E-12
5.50000	6.91150E+00	2.13878E-10	2.13878E-10	0.00000E+00	2.14960E-10
10.50000	1.31947E+01	7.82349E-10	7.82349E-10	0.00000E+00	7.83449E-10
15.50000	1.94779E+01	1.70614E-09	1.70614E-09	0.00000E+00	1.70724E-09
20.50000	2.57611E+01	2.98524E-09	2.98524E-09	0.00000E+00	2.98634E-09
25.50000	3.20442E+01	4.61964E-09	4.61964E-09	0.00000E+00	4.62075E-09
30.50000	3.83274E+01	6.60936E-09	6.60936E-09	0.00000E+00	6.61046E-09
35.50000	4.46106E+01	8.95435E-09	8.95435E-09	0.00000E+00	8.95548E-09
40.50000	5.08938E+01	1.16547E-08	1.16547E-08	0.00000E+00	1.16558E-08
45.50000	5.71770E+01	1.47103E-08	1.47103E-08	0.00000E+00	1.47114E-08
50.50000	6.34602E+01	1.81212E-08	1.81212E-08	0.00000E+00	1.81224E-08
55.50000	6.97434E+01	2.18873E-08	2.18873E-08	0.00000E+00	2.18886E-08
60.50000	7.60265E+01	2.60089E-08	2.60089E-08	0.00000E+00	2.60102E-08
65.50000	8.23097E+01	3.04858E-08	3.04858E-08	0.00000E+00	3.04870E-08
70.50000	8.85929E+01	3.53176E-08	3.53176E-08	0.00000E+00	3.53192E-08
75.50000	9.48761E+01	4.05039E-08	4.05039E-08	0.00000E+00	4.05066E-08
80.50000	1.01159E+02	4.60471E-08	4.60471E-08	0.00000E+00	4.60494E-08
85.50000	1.07442E+02	5.19455E-08	5.19455E-08	0.00000E+00	5.19475E-08
90.50000	1.13726E+02	5.81974E-08	5.81974E-08	0.00000E+00	5.82009E-08
95.50000	1.20009E+02	6.48068E-08	6.48068E-08	0.00000E+00	6.48095E-08
100.50000	1.26292E+02	7.17713E-08	7.17713E-08	0.00000E+00	7.17735E-08

TABLE 2. TABLE GENERATION MODE

m = 1.33333

RLO = 5.00000E-01. RHI = 1.05000E+02. DELR = 5.00000E+00
Wavelength = 5.00 m
Real Index = 1.33333000 Imag. Index = .00000000

R(m)	Size Parameter	Q(EXT)	Q(SCA)	Q(ABS)	ADF
.50000	6.28319E-01	4.44193E-02	4.44193E-02	0.00000E+00	8.68767E-02
5.50000	6.91150E+00	3.81237E+00	3.81237E+00	0.00000E+00	3.07148E+00
10.50000	1.31947E+01	2.33832E+00	2.33832E+00	0.00000E+00	1.82620E+00
15.50000	1.94779E+01	2.00868E+00	2.00868E+00	0.00000E+00	1.87679E+00
20.50000	2.57611E+01	2.56390E+00	2.56390E+00	0.00000E+00	2.24661E+00
25.50000	3.20442E+01	2.07078E+00	2.07078E+00	0.00000E+00	1.90576E+00
30.50000	3.83274E+01	2.05790E+00	2.05790E+00	0.00000E+00	1.93689E+00
35.50000	4.46106E+01	2.33004E+00	2.33004E+00	0.00000E+00	2.13875E+00
40.50000	5.08938E+01	2.14009E+00	2.14009E+00	0.00000E+00	1.93696E+00
45.50000	5.71770E+01	2.08112E+00	2.08112E+00	0.00000E+00	1.95759E+00
50.50000	6.34602E+01	2.24026E+00	2.24026E+00	0.00000E+00	2.09650E+00
55.50000	6.97434E+01	2.05988E+00	2.05988E+00	0.00000E+00	1.95275E+00
60.50000	7.60265E+01	2.06883E+00	2.06883E+00	0.00000E+00	1.96807E+00
65.50000	8.23097E+01	2.19703E+00	2.19703E+00	0.00000E+00	2.07396E+00
70.50000	8.85929E+01	2.04687E+00	2.04687E+00	0.00000E+00	1.96223E+00
75.50000	9.48761E+01	2.11949E+00	2.11949E+00	0.00000E+00	1.97440E+00
80.50000	1.01159E+02	2.16265E+00	2.16265E+00	0.00000E+00	2.05996E+00
85.50000	1.07442E+02	2.04734E+00	2.04734E+00	0.00000E+00	1.96855E+00
90.50000	1.13726E+02	2.05237E+00	2.05237E+00	0.00000E+00	1.97864E+00
95.50000	1.20009E+02	2.14777E+00	2.14777E+00	0.00000E+00	2.05041E+00
100.50000	1.26292E+02	2.04060E+00	2.04060E+00	0.00000E+00	1.97306E+00

TABLE 3. TABLE GENERATION MODE (CROSS-SECTIONS)
m = 1.0000015

RLO = 5.00000E-01. RHI = 4.50000E+01. DELR = 1.00000E+00
Wavelength = 15.00 m
Real Index = 1.00000150 Imag. Index = .00000000

	Size	Cross Sections in Square Meters			
R(m)	Parameter	Q(EXT)	Q(SCA)	Q(ABS)	ADF
.50000	2.09440E-01	5.93984E-15	5.93984E-15	0.00000E+00	1.55031E-13
1.50000	6.28319E-01	3.77008E-12	3.77008E-12	0.00000E+00	1.25575E-11
2.50000	1.04720E+00	6.18948E-11	6.18948E-11	0.00000E+00	9.68946E-11
3.50000	1.46608E+00	3.22713E-10	3.22713E-10	0.00000E+00	3.72230E-10
4.50000	1.88496E+00	9.61909E-10	9.61909E-10	0.00000E+00	1.01716E-09
5.50000	2.30383E+00	2.16275E-09	2.16275E-09	0.00000E+00	2.26981E-09
6.50000	2.72271E+00	4.24848E-09	4.24848E-09	0.00000E+00	4.42785E-09
7.50000	3.14159E+00	7.64968E-09	7.64968E-09	0.00000E+00	7.84846E-09
8.50000	3.56047E+00	1.27259E-08	1.27259E-08	0.00000E+00	1.29484E-08
9.50000	3.97935E+00	1.98716E-08	1.98716E-08	0.00000E+00	2.02038E-08
10.50000	4.39823E+00	2.97172E-08	2.97172E-08	0.00000E+00	3.01507E-08
11.50000	4.81711E+00	4.29363E-08	4.29363E-08	0.00000E+00	4.33841E-08
12.50000	5.23599E+00	6.00489E-08	6.00489E-08	0.00000E+00	6.05591E-08
13.50000	5.65487E+00	8.17080E-08	8.17080E-08	0.00000E+00	8.23900E-08
14.50000	6.07375E+00	1.08862E-07	1.08862E-07	0.00000E+00	1.09651E-07
15.50000	6.49262E+00	1.42374E-07	1.42374E-07	0.00000E+00	1.43175E-07
16.50000	6.91150E+00	1.82929E-07	1.82929E-07	0.00000E+00	1.83855E-07
17.50000	7.33038E+00	2.31494E-07	2.31494E-07	0.00000E+00	2.32644E-07
18.50000	7.74926E+00	2.89313E-07	2.89313E-07	0.00000E+00	2.90554E-07
19.50000	8.16814E+00	3.57389E-07	3.57389E-07	0.00000E+00	3.58656E-07
20.50000	8.58702E+00	4.36610E-07	4.36610E-07	0.00000E+00	4.38082E-07
21.50000	9.00590E+00	5.28296E-07	5.28296E-07	0.00000E+00	5.30021E-07
22.50000	9.42478E+00	6.33937E-07	6.33937E-07	0.00000E+00	6.35726E-07
23.50000	9.84366E+00	7.54649E-07	7.54649E-07	0.00000E+00	7.56504E-07
24.50000	1.02625E+01	8.91579E-07	8.91579E-07	0.00000E+00	8.93725E-07
25.50000	1.06814E+01	1.04642E-06	1.04642E-06	0.00000E+00	1.04882E-06
26.50000	1.11003E+01	1.22084E-06	1.22084E-06	0.00000E+00	1.22327E-06
27.50000	1.15192E+01	1.41606E-06	1.41606E-06	0.00000E+00	1.41863E-06
28.50000	1.19381E+01	1.63357E-06	1.63357E-06	0.00000E+00	1.63651E-06
29.50000	1.23569E+01	1.87541E-06	1.87541E-06	0.00000E+00	1.87857E-06
30.50000	1.27758E+01	2.14335E-06	2.14335E-06	0.00000E+00	2.14654E-06
31.50000	1.31947E+01	2.43877E-06	2.43877E-06	0.00000E+00	2.44220E-06
32.50000	1.36136E+01	2.76356E-06	2.76356E-06	0.00000E+00	2.76741E-06
33.50000	1.40324E+01	3.12004E-06	3.12004E-06	0.00000E+00	3.12406E-06
34.50000	1.44513E+01	3.51005E-06	3.51005E-06	0.00000E+00	3.51412E-06
35.50000	1.48702E+01	3.93519E-06	3.93519E-06	0.00000E+00	3.93961E-06
36.50000	1.52891E+01	4.39776E-06	4.39776E-06	0.00000E+00	4.40262E-06
37.50000	1.57080E+01	4.90033E-06	4.90033E-06	0.00000E+00	4.90529E-06
38.50000	1.61268E+01	5.44475E-06	5.44475E-06	0.00000E+00	5.44982E-06
39.50000	1.65457E+01	6.03294E-06	6.03294E-06	0.00000E+00	6.03848E-06
40.50000	1.69646E+01	6.66764E-06	6.66764E-06	0.00000E+00	6.67359E-06

TABLE 4. SINGLE TURBULE MODEL

$\lambda < \gamma$

m = 1.0000015

Wavelength = 5.00 m
Real Index = 1.00000150 Imag. Index = .00000000

R(m)	Size Parameter	Q(EXT)	Q(SCA)	Q(ABS)	ADF
30.00000	3.76991E+01	6.39439E-09	6.39439E-09	0.00000E+00	6.39550E-09

*** Phase Function (Integral over solid angle is unity) ***

Angle (Deg)	Phase Function	Angle (Deg)	Phase Function	Angle (Deg)	Phase Function
.000	1.00549E+02	.500	9.83923E+01	1.000	9.21591E+01
2.000	7.04779E+01	3.000	4.39194E+01	4.000	2.11377E+01
5.000	6.90125E+00	6.000	9.74323E-01	8.000	5.51044E-01
10.000	4.06732E-01	12.000	5.57109E-03	14.000	1.26362E-01
16.000	1.18102E-02	18.000	2.81551E-02	20.000	2.10238E-02
24.000	1.50308E-02	28.000	5.92785E-03	32.000	7.73665E-04
36.000	1.46115E-04	40.000	1.21146E-03	44.000	1.42367E-03
48.000	5.82885E-04	52.000	6.96884E-06	56.000	2.40956E-04
60.000	4.48025E-04	64.000	1.51021E-04	68.000	1.43342E-05
72.000	2.05845E-04	76.000	1.17420E-04	80.000	7.05946E-06
84.000	1.33905E-04	88.000	3.38229E-05	92.000	4.57344E-05
96.000	7.08101E-05	100.000	9.23468E-06	104.000	6.78840E-05
108.000	3.88159E-06	112.000	5.38492E-05	116.000	1.00587E-05
120.000	3.10136E-05	124.000	3.07702E-05	128.000	2.38710E-06
132.000	3.82840E-05	136.000	1.81152E-05	140.000	1.14544E-06
142.000	1.17876E-05	144.000	2.53459E-05	146.000	3.28441E-05
148.000	3.10271E-05	150.000	2.23238E-05	152.000	1.17272E-05
154.000	3.61213E-06	156.000	1.21887E-07	158.000	1.18045E-06
160.000	5.37666E-06	162.000	1.09503E-05	164.000	1.64533E-05
166.000	2.10105E-05	168.000	2.42952E-05	170.000	2.63621E-05
172.000	2.74691E-05	174.000	2.79327E-05	176.000	2.80440E-05
178.000	2.80226E-05	180.000	2.80014E-05		

Test integral of phase function is: 1.04217E+00

TABLE 5. SINGLE TURBULE MODEL

$\lambda < \gamma$

m = 1.33333

Wavelength = 5.00 m
Real Index = 1.33333000 Imag. Index = .00000000

R(m)	Size Parameter	Q(EXT)	Q(SCA)	Q(ABS)	ADF
30.00000	3.76991E+01	2.13171E+00	2.13171E+00	0.00000E+00	2.00004E+00

*** Phase Function (Integral over solid angle is unity) ***

Angle (Deg)	Phase Function	Angle (Deg)	Phase Function	Angle (Deg)	Phase Function
.000	6.19061E+01	.500	6.01188E+01	1.000	5.50098E+01
2.000	3.79818E+01	3.000	1.91703E+01	4.000	5.94872E+00
5.000	6.25238E-01	6.000	6.73745E-01	8.000	2.49006E+00
10.000	8.24598E-01	12.000	3.15137E-02	14.000	2.42282E-01
16.000	6.80251E-01	18.000	3.13066E-01	20.000	2.85330E-01
24.000	1.99759E-01	28.000	3.18359E-01	32.000	1.65788E-01
36.000	3.36434E-02	40.000	5.58591E-02	44.000	1.04645E-01
48.000	7.44567E-02	52.000	2.13933E-02	56.000	4.99427E-03
60.000	2.60021E-02	64.000	3.11628E-02	68.000	1.57804E-02
72.000	2.76854E-03	76.000	5.94687E-03	80.000	1.43038E-02
84.000	1.00182E-02	88.000	1.30953E-03	92.000	2.38238E-03
96.000	4.77071E-03	100.000	1.03444E-03	104.000	1.82243E-03
108.000	9.80708E-03	112.000	9.99972E-03	116.000	2.68559E-03
120.000	1.79242E-04	124.000	1.85665E-03	128.000	1.07126E-02
132.000	3.67086E-03	136.000	7.12088E-03	140.000	1.08049E-02
142.000	3.54139E-02	144.000	4.36453E-02	146.000	2.30289E-02
148.000	3.13271E-02	150.000	2.95026E-02	152.000	3.07851E-02
154.000	8.61732E-03	156.000	1.33666E-03	158.000	3.37359E-03
160.000	1.25980E-02	162.000	1.12088E-02	164.000	1.77247E-02
166.000	3.12651E-02	168.000	3.94053E-03	170.000	4.49724E-03
172.000	4.45448E-03	174.000	6.24914E-02	176.000	2.87252E-02
178.000	3.72092E-02	180.000	1.46867E-01		

Test integral of phase function is: 1.00015E+00

TABLE 6. SINGLE TURBULE MODEL

$\lambda < \gamma$

m = 1.0000015

Wavelength = 30.00 m
Real Index = 1.00000150 Imag. Index = .00000000

R(m)	Size Parameter	Q(EXT)	Q(SCA)	Q(ABS)	ADF
5.00000	1.04720E+00	3.15228E-12	3.15228E-12	0.00000E+00	4.93480E-12

*** Phase Function (Integral over solid angle is unity) ***

Angle (Deg)	Phase Function	Angle (Deg)	Phase Function	Angle (Deg)	Phase Function
.000	1.21434E-01	.500	1.21432E-01	1.000	1.21426E-01
2.000	1.21402E-01	3.000	1.21361E-01	4.000	1.21305E-01
5.000	1.21232E-01	6.000	1.21143E-01	8.000	1.20917E-01
10.000	1.20627E-01	12.000	1.20275E-01	14.000	1.19861E-01
16.000	1.19386E-01	18.000	1.18851E-01	20.000	1.18258E-01
24.000	1.16903E-01	28.000	1.15335E-01	32.000	1.13568E-01
36.000	1.11619E-01	40.000	1.09507E-01	44.000	1.07250E-01
48.000	1.04868E-01	52.000	1.02381E-01	56.000	9.98096E-02
60.000	9.71734E-02	64.000	9.44920E-02	68.000	9.17842E-02
72.000	8.90681E-02	76.000	8.63606E-02	80.000	8.36776E-02
84.000	8.10337E-02	88.000	7.84423E-02	92.000	7.59153E-02
96.000	7.34634E-02	100.000	7.10959E-02	104.000	6.88210E-02
108.000	6.66455E-02	112.000	6.45751E-02	116.000	6.26145E-02
120.000	6.07673E-02	124.000	5.90365E-02	128.000	5.74241E-02
132.000	5.59315E-02	136.000	5.45596E-02	140.000	5.33089E-02
142.000	5.27291E-02	144.000	5.21795E-02	146.000	5.16601E-02
148.000	5.11710E-02	150.000	5.07120E-02	152.000	5.02831E-02
154.000	4.98842E-02	156.000	4.95153E-02	158.000	4.91762E-02
160.000	4.88669E-02	162.000	4.85873E-02	164.000	4.83374E-02
166.000	4.81170E-02	168.000	4.79262E-02	170.000	4.77648E-02
172.000	4.76329E-02	174.000	4.75303E-02	176.000	4.74570E-02
178.000	4.74131E-02	180.000	4.73984E-02		

Test integral of phase function is: 1.00005E+00

TABLE 7. SINGLE TURBULE MODEL

$\lambda < \gamma$

m = 1.33333

Wavelength = 30.00 m
Real Index = 1.33333000 Imag. Index = .00000000

R(m)	Size Parameter	Q(EXT)	Q(SCA)	Q(ABS)	ADF
5.00000	1.04720E+00	3.08358E-01	3.08358E-01	0.00000E+00	2.37171E-01

*** Phase Function (Integral over solid angle is unity) ***

Angle (Deg)	Phase Function	Angle (Deg)	Phase Function	Angle (Deg)	Phase Function
.000	1.16616E-01	.500	1.16615E-01	1.000	1.16609E-01
2.000	1.16588E-01	3.000	1.16553E-01	4.000	1.16503E-01
5.000	1.16439E-01	6.000	1.16361E-01	8.000	1.16164E-01
10.000	1.15910E-01	12.000	1.15602E-01	14.000	1.15240E-01
16.000	1.14824E-01	18.000	1.14356E-01	20.000	1.13836E-01
24.000	1.12650E-01	28.000	1.11275E-01	32.000	1.09725E-01
36.000	1.08015E-01	40.000	1.06160E-01	44.000	1.04176E-01
48.000	1.02081E-01	52.000	9.98906E-02	56.000	9.76235E-02
60.000	9.52967E-02	64.000	9.29272E-02	68.000	9.05313E-02
72.000	8.81250E-02	76.000	8.57231E-02	80.000	8.33397E-02
84.000	8.09876E-02	88.000	7.86789E-02	92.000	7.64244E-02
96.000	7.42336E-02	100.000	7.21151E-02	104.000	7.00765E-02
108.000	6.81240E-02	112.000	6.62631E-02	116.000	6.44984E-02
120.000	6.28336E-02	124.000	6.12714E-02	128.000	5.98142E-02
132.000	5.84636E-02	136.000	5.72208E-02	140.000	5.60865E-02
142.000	5.55601E-02	144.000	5.50610E-02	146.000	5.45891E-02
148.000	5.41445E-02	150.000	5.37271E-02	152.000	5.33369E-02
154.000	5.29739E-02	156.000	5.26379E-02	158.000	5.23291E-02
160.000	5.20473E-02	162.000	5.17926E-02	164.000	5.15647E-02
166.000	5.13638E-02	168.000	5.11898E-02	170.000	5.10426E-02
172.000	5.09222E-02	174.000	5.08286E-02	176.000	5.07618E-02
178.000	5.07217E-02	180.000	5.07083E-02		

Test integral of phase function is: 1.00004E+00

TABLE 8. ARBITRARY USER-SUPPLIED MODEL

m = 1.0000015

Radius	Relative No.	Radius	Relative No.	Radius	Relative No.
1.900000E-01	1.000000E+00	2.500000E-01	1.000000E+00	3.000000E-01	1.000000E+00
3.500000E-01	1.000000E+00	4.000000E-01	1.000000E+00		

Average numerical dry volume per particle is: 1.211598E-01 cubic meters

Wavelength = .11 m
Real Index = 1.00000150
Imag. Index = .00000000
Number Density = 2.10000E-01 part/cubic meter

Size Group	Maximum Radius	Group cross sections in square meters per particle			
		Extinction	Absorption	Scattering	Backscatter
1	.400	4.38812E-10	4.48416E-44	4.38812E-10	3.18346E-13

*** Phase Function (integral over solid angle is unity) ***

Angle (Deg)	Phase Function	Angle (Deg)	Phase Function	Angle (Deg)	Phase Function
.000	2.69153E+01	2.813	2.20677E+01	5.625	1.18638E+01
8.438	3.84435E+00	11.250	6.91398E-01	14.063	2.09543E-01
16.875	1.54649E-01	19.688	6.20410E-02	22.500	3.56652E-02
25.313	3.06032E-02	28.125	1.63331E-02	30.938	1.10230E-02
33.750	9.18239E-03	36.563	5.49717E-03	39.375	4.27419E-03
42.188	3.85865E-03	45.000	2.64059E-03	47.813	2.11049E-03
50.625	1.89161E-03	53.438	1.36339E-03	56.250	1.10207E-03
59.063	1.04922E-03	61.875	8.42690E-04	64.688	6.78473E-04
67.500	6.40439E-04	70.313	5.48956E-04	73.125	4.33446E-04
75.938	3.97018E-04	78.750	3.76826E-04	81.563	3.19339E-04
84.375	2.75281E-04	87.188	2.63894E-04	90.000	2.44566E-04
92.813	2.08157E-04	95.625	1.83319E-04	98.438	1.76756E-04
101.250	1.68788E-04	104.063	1.51246E-04	106.875	1.35169E-04
109.688	1.28484E-04	112.500	1.25767E-04	115.313	1.19032E-04
118.125	1.08046E-04	120.938	9.81422E-05	123.750	9.28082E-05
126.563	9.08515E-05	129.375	8.90175E-05	132.188	8.53915E-05
135.000	8.03582E-05	137.813	7.54421E-05	140.625	7.18429E-05
143.438	6.98105E-05	146.250	6.88598E-05	149.063	6.82929E-05
151.875	6.75910E-05	154.688	6.65425E-05	157.500	6.51827E-05
160.313	6.36674E-05	163.125	6.21686E-05	165.938	6.08176E-05
168.750	5.96912E-05	171.563	5.88209E-05	174.375	5.82100E-05
177.188	5.78500E-05	180.000	5.77313E-05		

Test integral of phase function is: 1.06681E+00

TABLE 9. ARBITRARY USER-SUPPLIED MODEL

m = 1.33333

Radius	Relative No.	Radius	Relative No.	Radius	Relative No.
1.900000E-01	1.000000E+00	2.500000E-01	1.000000E+00	3.000000E-01	1.000000E+00
3.500000E-01	1.000000E+00	4.000000E-01	1.000000E+00		

Average numerical dry volume per particle is: 1.211598E-01 cubic meters

---

Wavelength = .11 m
Real Index = 1.33333000
Imag. Index = .00000000
Number Density = 2.10000E-01 part/cubic meter

Size Group	Maximum Radius	Group cross sections in square meters per particle			
		Extinction	Absorption	Scattering	Backscatter
1	.400	6.42572E-01	0.00000E+00	6.42572E-01	1.76685E+00

*** Phase Function (integral over solid angle is unity) ***

Angle (Deg)	Phase Function	Angle (Deg)	Phase Function	Angle (Deg)	Phase Function
.000	1.56191E+01	2.813	1.19070E+01	5.625	5.20701E+00
8.438	1.55340E+00	11.250	8.72676E-01	14.063	6.94558E-01
16.875	4.63789E-01	19.688	3.92105E-01	22.500	3.25768E-01
25.313	2.19202E-01	28.125	1.78952E-01	30.938	1.68788E-01
33.750	1.32202E-01	36.563	1.08059E-01	39.375	9.91544E-02
42.188	7.95723E-02	45.000	6.49130E-02	47.813	5.96756E-02
50.625	4.94084E-02	53.438	4.11315E-02	56.250	3.74403E-02
59.063	2.99048E-02	61.875	2.49234E-02	64.688	2.31956E-02
67.500	1.85913E-02	70.313	1.60056E-02	73.125	1.50842E-02
75.938	1.17547E-02	78.750	9.95956E-03	81.563	9.55965E-03
84.375	7.62468E-03	87.188	6.84997E-03	90.000	6.63866E-03
92.813	5.49053E-03	95.625	5.30885E-03	98.438	5.31182E-03
101.250	5.21668E-03	104.063	5.40052E-03	106.875	5.47881E-03
109.688	5.56325E-03	112.500	5.45785E-03	115.313	5.58924E-03
118.125	6.15020E-03	120.938	6.34299E-03	123.750	6.35298E-03
126.563	7.99460E-03	129.375	9.02378E-03	132.188	1.10437E-02
135.000	1.53470E-02	137.813	1.62270E-02	140.625	2.27691E-02
143.438	2.94942E-02	146.250	2.78958E-02	149.063	3.62969E-02
151.875	3.89313E-02	154.688	2.87069E-02	157.500	2.53064E-02
160.313	1.94413E-02	163.125	1.45743E-02	165.938	1.49503E-02
168.750	2.14306E-02	171.563	2.16007E-02	174.375	3.05357E-02
177.188	1.32714E-01	180.000	2.18811E-01		

Test integral of phase function is: 1.03898E+00

TABLE 10. LOG-NORMAL SIZE DISTRIBUTION MODEL

m = 1.0000015

RBAR = 2.25000E-01. SIGMA = 8.00000E-02. RLO = 2.00000E-01
RHI = 6.50000E-01. DENS = 5.00000E+00

Average numerical dry volume per particle is: 3.086332E-01 cubic meters

---

Wavelength = .12 m
Real Index = 1.00000150
Imag. Index = .00000000
Number Density = 5.00000E+00 part/cubic meter

Size Group	Maximum Radius	Group cross sections in square meters per particle			
		Extinction	Absorption	Scattering	Backscatter
1	.650	1.41035E-09	0.00000E+00	1.41035E-09	5.63142E-13

*** Phase Function (Integral over solid angle is unity) ***

Angle (Deg)	Phase Function	Angle (Deg)	Phase Function	Angle (Deg)	Phase Function
.000	5.46813E+01	2.813	3.57618E+01	5.625	9.18735E+00
8.438	1.11536E+00	11.250	4.41477E-01	14.063	1.31935E-01
16.875	7.58641E-02	19.688	3.32985E-02	22.500	2.35993E-02
25.313	1.31178E-02	28.125	9.94893E-03	30.938	6.10393E-03
33.750	4.71830E-03	36.563	3.12050E-03	39.375	2.54196E-03
42.188	1.82794E-03	45.000	1.55004E-03	47.813	1.15871E-03
50.625	9.90197E-04	53.438	7.55367E-04	56.250	6.57504E-04
59.063	5.22778E-04	61.875	4.64370E-04	64.688	3.85438E-04
67.500	3.38978E-04	70.313	2.91634E-04	73.125	2.50455E-04
75.938	2.24592E-04	78.750	1.92143E-04	81.563	1.76692E-04
84.375	1.55715E-04	87.188	1.40705E-04	90.000	1.29404E-04
92.813	1.14679E-04	95.625	1.06163E-04	98.438	9.71798E-05
101.250	8.78992E-05	104.063	8.25674E-05	106.875	7.66793E-05
109.688	7.05860E-05	112.500	6.67580E-05	115.313	6.30485E-05
118.125	5.86993E-05	120.938	5.53438E-05	123.750	5.28847E-05
126.563	5.02146E-05	129.375	4.74549E-05	132.188	4.52723E-05
135.000	4.36412E-05	137.813	4.21141E-05	140.625	4.05212E-05
143.438	3.90216E-05	146.250	3.77783E-05	149.063	3.67912E-05
151.875	3.59630E-05	154.688	3.52097E-05	157.500	3.45032E-05
160.313	3.38544E-05	163.125	3.32842E-05	165.938	3.28063E-05
168.750	3.24241E-05	171.563	3.21348E-05	174.375	3.19330E-05
177.188	3.18140E-05	180.000	3.17748E-05		

Test integral of phase function is: 1.13438E+00

TABLE 11. LOG-NORMAL SIZE DISTRIBUTION MODEL

m = 1.33333

RBAR = 2.25000E-01. SIGMA = 8.00000E-02. RLO = 2.00000E-01
RHI = 6.50000E-01. DENS = 5.00000E+00

Average numerical dry volume per particle is: 3.086332E-01 cubic meters

---

Wavelength = .12 m
Real Index = 1.33333000
Imag. Index = .00000000
Number Density = 5.00000E+00 part/cubic meter

Size Group	Maximum Radius	Group cross sections in square meters per particle			
		Extinction	Absorption	Scattering	Backscatter
1	.650	1.11976E+00	0.00000E+00	1.11976E+00	2.59044E+00

*** Phase Function (Integral over solid angle is unity) ***

Angle (Deg)	Phase Function	Angle (Deg)	Phase Function	Angle (Deg)	Phase Function
.000	2.79135E+01	2.813	1.68235E+01	5.625	3.92475E+00
8.438	1.28005E+00	11.250	7.36541E-01	14.063	5.85671E-01
16.875	4.29428E-01	19.688	3.47377E-01	22.500	2.89255E-01
25.313	2.35830E-01	28.125	2.02544E-01	30.938	1.61005E-01
33.750	1.42696E-01	36.563	1.16183E-01	39.375	9.90076E-02
42.188	7.84624E-02	45.000	6.84321E-02	47.813	5.42196E-02
50.625	4.72283E-02	53.438	3.81453E-02	56.250	3.31485E-02
59.063	2.71950E-02	61.875	2.27121E-02	64.688	1.86862E-02
67.500	1.62634E-02	70.313	1.33752E-02	73.125	1.15372E-02
75.938	9.96603E-03	78.750	8.47404E-03	81.563	7.61079E-03
84.375	6.65180E-03	87.188	5.57197E-03	90.000	5.58129E-03
92.813	4.37463E-03	95.625	4.36005E-03	98.438	4.07728E-03
101.250	3.96532E-03	104.063	4.19893E-03	106.875	4.33502E-03
109.688	4.54302E-03	112.500	4.82269E-03	115.313	5.15307E-03
118.125	5.38522E-03	120.938	5.35189E-03	123.750	6.11372E-03
126.563	6.90978E-03	129.375	8.13378E-03	132.188	1.15220E-02
135.000	1.31309E-02	137.813	2.00602E-02	140.625	2.26719E-02
143.438	2.79511E-02	146.250	3.40878E-02	149.063	3.29420E-02
151.875	2.90356E-02	154.688	2.12366E-02	157.500	1.47333E-02
160.313	1.38721E-02	163.125	1.02886E-02	165.938	2.00481E-02
168.750	1.78127E-02	171.563	1.67157E-02	174.375	2.12180E-02
177.188	8.56301E-02	180.000	1.84094E-01		

Test integral of phase function is: 1.06846E+00

Literature Cited

Abramowitz, M., and I. A. Stegun, Eds., 1970, Handbook of Mathematical Functions, Applied Mathematics Series 55, Chaps. 8, 10, U.S. Government, Printing Office, Washington, D.C.

Bohren, Craig F., 1983, Absorption and Scattering of Light by Small Particles, John Wiley & Sons.

Lentz, William J., 1976, Generating Bessel Functions in Mie Scattering Calculations Using Continued Fractions, Applied Optics, 15:3.

Miller, August, 1983, Mie Code AGAUS 82, ASL-CR-83-0100-3, U.S. Army Atmospheric Sciences Laboratory, White Sands Missile Range, New Mexico.

Morse, Philip M., and K. U. Ingard, 1968, Theoretical Acoustics, McGraw-Hill Book Company.

Nguyen, X. Nguyen, 1993, Conversion of AGAUS Single Precision Code to Quadruple Precision Code, Contract No. DAAD0791M0664, U.S. Army Research Laboratory, White Sands Missile Range, New Mexico.

Noble, John W., and Harry J. Auvermann (Draft), 1993, The Effect of Large and Small Scale Turbulence on Sound Propagation in the Atmosphere, Battlefield Environment Directorate, U.S. Army Research Laboratory, White Sands Missile Range, New Mexico 88002-5501.

Van de Hulst, H.C., 1957, Light Scattering by Spherical Particles, John Wiley & Sons, Inc.

Appendix A. Notes on Acoustic Scattering by a Spherical Turbule

Dr. G. H. Goedecke
Department of Physics
New Mexico State University
Las Cruces, New Mexico 88003

The problem of acoustic scattering by a spherical turbule having uniform reference density different from that of the surroundings but having no flow velocity is solved in these notes. Complete analytic solutions for the differential and total cross-sections for an ideal fluid (no viscosity) are given. The analytic expressions can be evaluated easily if subroutines are available that generate values of spherical Bessel and Neumann functions ($j_\ell(x)$, $n_\ell(x)$) for given arguments x and that calculate values of the Legendre polynomials $P_\ell(\mu)$ for given argument μ for integers $\ell \geq 0$. These subroutines exist in any Mie scattering code. In the following, bold symbols such as **r** are three vectors.

1. General Equations and Boundary Conditions

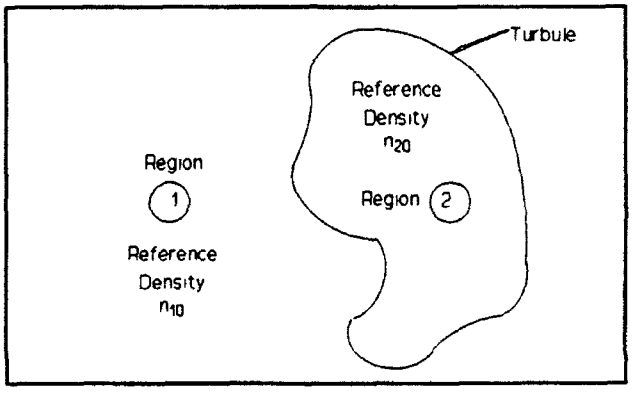

Figure A-1. Constituents of the propagation region.

Referring to figure A-1, imagine a massless but perfectly insulating membrane separating the two regions. Then the pressure must be continuous across the membrane; otherwise, the massless membrane would experience infinite acceleration. If the pressure is continuous, then the massless membrane will not be deformed.

Then, in the reference condition with no waves present, we have

$$p_{10} = n_{10}k_B T_{10} = p_{20} = n_{20}k_B T_{20} = p_0, \tag{A-1}$$

$$p_{10} = n_{10}k_B T_{10} = p_{20} = n_{20}k_B T_{20} = p_0, \tag{A-1}$$

where n_{10}, n_{20} are the reference number concentrations in regions 1 and 2, respectively; p_{10}, p_{20}, p_0 are pressures; T_{10}, T_{20} are absolute temperatures; and k_B is the Boltzmann constant. Thus, if the reference number densities are different, then the temperatures must be different.

Now, consider small adiabatic disturbances away from these reference conditions. Then, we have

$$p_1 = p_0 n_1^\gamma / n_{10}^\gamma \quad ; \quad p_2 = p_0 n_2^\gamma / n_{20}^\gamma, \tag{A-2}$$

where γ is the ratio of specific heats. Now, let

$$n_1 = n_{10}(1 + e_1(r,t)) \quad ; \quad n_2 = n_{20}(1 + e_2(r,t)). \tag{A-3}$$

Then, equations (A-2), (A-3), and continuity of pressure across the boundary imply

$$e_1 = e_2 \tag{A-4}$$

at the boundary, or $\epsilon(\mathbf{r},t)$ is continuous across a boundary.

In each region, we have the equations

$$\frac{\partial n}{\partial t} + \nabla \cdot (n\mathbf{v}) = 0 \tag{A-5}$$

$$\frac{\partial \mathbf{v}}{\partial t} + \mathbf{v} \cdot \nabla \mathbf{v} = -\frac{1}{Mn}\nabla p \tag{A-6}$$

where M = mass of molecule.

Equation (A-5) implies that $n_{10}\, v_{1\perp}$ is continuous. To first order in small quantities, regarding v as small, this requires

$$n_{10} v_{1\perp} = n_{20} v_{2\perp} \tag{A-7}$$

at the boundary, or $n_0 v_\perp$ is continuous across the boundary.

Now, linearize equations (A-5) and (A-6) using

$$p = p_0(1 + \gamma e) \tag{A-8}$$

in each region. Then equations (A-5) and (A-6) yield

$$\frac{\partial e}{\partial t} + \nabla \cdot v = 0, \tag{A-9}$$

$$\begin{aligned} \frac{\partial v}{\partial t} &= -\frac{p_0 \gamma}{M n_0} \nabla e = -c^2 \nabla e , \\ c^2 &= \frac{\gamma p_0}{M n_0} = \frac{\gamma k_B T_0}{M}. \end{aligned} \tag{A-10}$$

Putting in a time dependence $e^{-i\omega t}$, we have

$$e = \frac{1}{i\omega} \nabla \cdot v \tag{A-11}$$

$$v = \frac{c^2}{i\omega} \nabla e. \tag{A-12}$$

Now, from equation (A-7), with $\hat{n}$ ≡ outward unit normal to boundary surface at any point on the surface, we have, with equation (A-10)

$$n_{10}v_{1\perp} = \frac{n_{10}c_1^2}{i\omega}\,\hat{n}\cdot\nabla e_1 = \frac{p_0\gamma}{i\omega M}\,\hat{n}\cdot\nabla e_1,$$
$$n_{20}v_{2\perp} = \frac{n_{20}c_2^2}{i\omega}\,\hat{n}\cdot\nabla e_2 = \frac{p_0\gamma}{i\omega M}\,\hat{n}\cdot\nabla e_2. \qquad \text{(A-13)}$$

From this, we see immediately that

$$\hat{n}\cdot\nabla e_1 = \hat{n}\cdot\nabla e_2 \qquad \text{(A-14)}$$

at the boundary, or $\hat{n}\cdot\Delta e$ is continuous across the boundary.

Combining equations (A-11) and (A-12), we have

$$\Delta^2 e_1 + k^2 e_1 = 0\ ,\quad \Delta^2 e_2 + m^2 k^2 e_2 = 0, \qquad \text{(A-15)}$$

where

$$k = \frac{\omega}{c_1},\qquad m = \frac{c_1}{c_2}, \qquad \text{(A-16)}$$

and m = "refractive index" of region 2 with respect to region 1.

Thus, we have to solve equation (A-15), subject to the boundary conditions (A-4) and (A-14); that is,

$$\begin{aligned} &e \text{ is continuous across the boundary,}\\ &\hat{n}\cdot\nabla e \text{ is continuous across the boundary.}\end{aligned} \qquad \text{(A-17)}$$

These are exactly the same conditions and equations that apply for potential scattering by a uniform potential in quantum mechanics; ϵ here corresponds to the wave function in quantum mechanics.

2. Application to a Spherical Region

We let region 2 be a sphere of radius a centered at the origin. We assume a plane wave of unit amplitude incident in the z-direction:

$$e_0(r) = e^{ikz} = \sum_{\ell=0}^{\infty} (2\ell + 1) i^{\ell} j_{\ell}(kr) P_{\ell}(\cos\theta). \tag{A18}$$

The second equality expresses the plane wave in terms of the spherical Bessel function $j_\ell(kr)$ and the Legendre function $P_\ell(\cos\theta)$. So we write

$$e_1(r,\theta) = \sum_{\ell=0}^{\infty} (2\ell + 1) i^{\ell} [j_{\ell}(kr) + a_{\ell} h_{\ell}^{(1)}(kr)] P_{\ell}(\cos\theta) \tag{A-19}$$

$$e_2(r,\theta) = \sum_{\ell=0}^{\infty} (2\ell + 1) i^{\ell} b_{\ell} j_{\ell}(mkr) P_{\ell}(\cos\theta), \tag{A-20}$$

as the general solutions of equation (A-15) in regions 1 and 2, respectively. The coefficients (a_ℓ ,b_ℓ) are to be determined using the boundary conditions (A-17), which for a sphere are

$$e_1(a,\theta) = e_2(a,\theta) \tag{A-21}$$

$$\frac{\partial e_1}{\partial r}(a,\theta) = \frac{\partial e_2}{\partial r}(a,\theta). \tag{A-22}$$

The scattered wave is the second term in equation (A-19). For $r \to \infty$, we know that

$$h_{\ell}^{(1)}(kr) \underset{r\to\infty}{\sim} (-i)^{\ell+1} \frac{e^{ikr}}{kr}, \tag{A-23}$$

so the scattered wave is

$$e_s(r,\theta) \underset{r\to\infty}{\sim} \frac{e^{ikr}}{r} \cdot \frac{1}{ik}\sum_{\ell=0}^{\infty}(2\ell + 1)a_\ell P_\ell(\cos\theta), \tag{A-24}$$

whereby the scattering amplitude f(k,θ) is

$$f(k,\theta) = \frac{1}{ik}\sum_{\ell=0}^{\infty}(2\ell + 1)a_\ell P_\ell(\cos\theta). \tag{A-25}$$

The differential scattering cross-section is

$$\sigma(k,\theta) = |f(k,\theta)|^2. \tag{A-26}$$

The total scattering cross-section may be obtained in two ways.

First,

$$\sigma_s(k) = \frac{2\pi}{k^2}\sum_{\ell}\sum_{\ell'}(2\ell + 1)(2\ell' + 1)a_\ell a^*_{\ell'}\int_0^{\pi} d\theta \sin\theta P_\ell(\cos\theta)P_{\ell'}(\cos\theta). \tag{A-27}$$

But the integral is equal to

$$\delta_{\ell\ell'}\frac{2}{2\ell'+1}, \tag{A-28}$$

where $\delta_{\ell\ell'}$ is the Kronecker delta. So

$$\sigma_s(k) = \frac{4\pi}{k^2}\sum_{\ell=0}^{\infty}(2\ell + 1)|a_\ell|^2. \tag{A-29}$$

The optical theorem yields the extinction cross-section

$$\sigma_e(k) = \frac{4\pi}{k}\Im m(f(0^\circ)) = \frac{4\pi}{k^2}\sum_{\ell=0}^{\infty}(2\ell + 1)\Im m(-ia_\ell),$$
$$\sigma_e(k) = -\frac{4\pi}{k^2}\sum_{\ell=0}^{\infty}(2\ell + 1)\Re e(a_\ell) \qquad \text{(A-30)}$$

since $P_\ell(\cos 0^\circ) = 1$, for all ℓ, and $\Im m(-ia_\ell) = \Im m(-i\Re e(a_\ell) + \Im m(a_\ell)) = -\Re e(a_\ell)$.

If the refractive index of region 2 is real, as it is here, then we should have

$$\sigma_e(k) = \sigma_s(k). \qquad \text{(A-31)}$$

So, once we have found the a_ℓ, we can evaluate $f(k,\theta)$, $\sigma(k,\theta)$, and σ_s. In order to find the a_ℓ, we apply the boundary conditions (A-21) and (A-22) to equations (A-19) and (A-20). This yields

$$j_\ell(ka) + a_\ell h_\ell^{(1)}(ka) = b_\ell j_\ell(mka), \qquad \text{(A-32)}$$

$$j_\ell'(ka) + a_\ell h_\ell^{(1)\prime}(ka) = mb_\ell j_\ell'(mka). \qquad \text{(A-33)}$$

Here, the prime means "derivative with respect to the argument."

Solution of these equations for a_ℓ yields,

$$\frac{1}{a_\ell} = -\frac{j_\ell(mx)h_\ell^{(1)\prime}(x) - mj_\ell'(mx)h_\ell^{(1)}(x)}{j_\ell(mx)j_\ell'(x) - mj_\ell'(mx)j_\ell(x)}, \qquad \text{(A-34)}$$

where

$$x = ka. \qquad \text{(A-35)}$$

Since $h_\ell^{(1)} = j_\ell + in_\ell$, we have

$$\frac{1}{a_\ell} = -\left(1 + i\frac{j_\ell(mx)n_\ell'(x) - mj_\ell'(mx)n_\ell(x)}{j_\ell(mx)j_\ell'(x) - mj_\ell'(mx)j_\ell(x)}\right),$$

$$= -1 - \Gamma_\ell \tag{A-36}$$

where Γ_ℓ is the ratio above, and is real for real m. Thus

$$a_\ell = -\frac{1}{1 + i\Gamma_\ell} = -\frac{(1 - i\Gamma_\ell)}{1 + \Gamma_\ell^2}. \tag{A-37}$$

Therefore,

$$-\Re e(a_\ell) = \frac{1}{1 + \Gamma_\ell^2} = |\, a_\ell \,|^2. \tag{A-38}$$

From equations (A-38), (A-30), and (A-29), we see that indeed

$$\sigma_s = \frac{4\pi}{k^2}\sum_{\ell=0}^{\infty}(2\ell + 1)\left(\frac{1}{1 + \Gamma_\ell^2}\right) = \sigma_s \tag{A-39}$$

where

$$\Gamma_\ell = \frac{j_\ell(mx)n_\ell'(x) - mj_\ell'(mx)n_\ell(x)}{j_\ell(mx)j_\ell'(x) - mj_\ell'(mx)j_\ell(x)}. \tag{A-40}$$

Depending on m and x = ka, $\Gamma_\ell \to 0$ for some $\ell > \ell_{max}$; that is, we can neglect $\ell > \ell_{max}$. The larger m and the larger ka, the larger ℓ_{max}. Roughly, $\ell_{max} \approx$ mka. So for computational purposes, we take all sums from $\ell = 0$ to ℓ_{max}.

For example, suppose mka $\ll 1$. Then the dominant term is $\ell = 0$, and we get

$$f(k,\theta) = -\frac{1}{ik} \cdot \frac{1}{1 + i\Gamma_0} \quad , \quad \sigma(k,\theta) = \frac{1}{k^2(1 + \Gamma_0^2)} \tag{A-41}$$

independent of θ; so the scattering is especially symmetric (monopole). This is to be contrasted with the lowest order multipole for the corresponding electromagnetic wave problem, which is dipole in character, with $\sigma(k,\theta)$ dependent on θ.

For this case, mka $\ll$ 1, we can evaluate Γ_0 easily. We need only the asymptotic forms of (j_0, n_0) for small argument.

From equations (A-12) and (A-24), we see that the scattered wave velocity field is given in the radiation zone ($r \to \infty$) by

$$v_s(r,\theta) = \frac{c_1^2}{i\omega}\nabla e_s(r,\theta) \underset{r\to\infty}{\sim} \frac{e^{ikr}}{r} \hat{r}\, c_1 f(k,\theta). \tag{A-42}$$

Thus, the fluid velocity of the scattered wave is radial (longitudinal). This is to be contrasted with the electric and magnetic fields in the scattered wave in an electromagnetic scattering problem, which are transverse to $\hat{r}$.

At any rate, we have a complete analytic solution to the problem of scattering of acoustic waves by a sphere of uniform reference density different from that of the surroundings. Merely evaluate the Γ_ℓ, $\ell = 0, \ell_{max}$ using standard algorithms for the spherical Bessel and Neumann functions (j_ℓ, n_ℓ); then substitute the results into equation (A-37) for a_ℓ, then substitute a_ℓ into equation (A-25) for $f(k,\theta)$ using standard algorithms to evaluate the Legendre functions $P_\ell(\cos\theta)$.

Appendix B. The Four Size Distribution Models of ASCT

Type 0: Arbitrary User-Supplied Discrete Model

This distribution type allows the user to enter from 1 to 513 pairs of data. NRADI is the pairs of radii and absolute number densities. The radius must be entered in meters and the absolute number density in particles per cubic meter per meter. The input file has the following format:

NWAVE NIDSTP ICQ NANG IANG NBINS IEO NEOU NUNIT MQRTE
DELTA ATOP (if IDELT = 1)
IDSTP NRADI 0. 0. 0. 0. 0.
R1 F(R1)
R2 F(R2)
.
.
RNRADI F(RNRADI)
WAVE EM CAY 0. 0. 0. 0. 0.

Type 1: Log-Normal Distribution Model

This model is used to compute the cross-sections and phase function for a log-normal distribution of turbule sizes and is described by the following formula:

$$f(r) = \frac{C}{r}\exp\{-\frac{1}{2}[\frac{|\ln(r/\bar{r})|}{\ln(\sigma)}]^2\}. \qquad \text{(B-1)}$$

The input file has the following format:

NWAVE NIDSTP ICQ NANG IANG NBINS IEO NEOU NUNIT MQRTE
DELTA ATOP (if IDELT = 1)
IDSTP RLO RHI RBAR SIGMA DENS
WAVE EM CAY 0. 0. 0. 0. 0.

RLO - The minimum radius (m) at which the model is to be cutoff.
RHI - The maximum radius (m) at which the model is to be cutoff.
RBAR - The radius (m) at which the relative number density peaks.
SIGMA - The standard deviation to be used (not LN(SIGMA)).
DENS - The number of particles per cubic meter.

Type 2: Single Turbule Model: Efficiency Factors/Cross-Sections
Phase Function Calculations

Used to compute efficiency factors (ICQ = 0) or cross-sections (ICQ = 1) and phase function for a single turbule radius. The input file has the following format:

NWAVE NIDSTP ICQ NANG IANG NBINS IEO NEOU NUNIT MQRTE
DELTA ATOP (if IDELT = 1)
IDSTP RADIUS 0. 0. 0. 0. 0.
WAVE EM CAY 0. 0. 0. 0.

Type 3: Special Table Generation Mode

This is not a distribution model but is an operating model used for calculating and printing tables of the efficiency factors as a function of radius. The input file has the following format:

NWAVE NIDSTP ICQ NANG IANG NBINS IEO NEOU NUNIT MQRTE
DELTA ATOP (if IDELT = 1)
IDSTP RLO RHI DELR 0. 0. 0.
WAVE EM CAY 0. 0. 0. 0. 0.

RLO - The minimum turbule radius (m) to be used.
RHI - The maximum turbule radius (m) to be used.
DELR - The increment in radius (m) to be used.

Appendix C. AGAUS Formulas

The formulas implemented in program AGAUS for calculating the efficiency factors and the phase function are given below. They are included here to compare the corresponding acoustic formulas for efficiency factors and phase function more easily.

Expansion Coefficients

$$a_\ell = \frac{[\frac{A_\ell(mx)}{m} + \frac{\ell}{x}]\Re e[\xi_\ell(x)] - \Re e[\xi_{\ell-1}(x)]}{[\frac{A_\ell(mx)}{m} + \frac{\ell}{x}]\xi_\ell(x) - \xi_{\ell-1}(x)}, \tag{C-1}$$

$$b_\ell = \frac{[mA_\ell(mx) + \frac{\ell}{x}]\Re e[\xi_\ell(x)] - \Re e[\xi_{\ell-1}(x)]}{[mA_\ell(mx) + \frac{\ell}{x}]\xi_\ell(x) - \xi_{\ell-1}(x)}, \tag{C-2}$$

$$A_\ell(mx) = -\frac{\ell}{mx} + \frac{j_{\ell-1}(mx)}{j_\ell(mx)} \tag{C-3}$$

Efficiency Factors

$$Q_{ext} = \frac{2}{x^2}\sum_{\ell=1}^{\infty}(2\ell + 1)\Re e(a_\ell + b_\ell) \tag{C-4}$$

$$Q_{sca} = \frac{2}{x^2}\sum_{\ell=1}^{\infty}(2\ell + 1)[|\, a_\ell|^2 + |\, b_\ell|^2] \tag{C-5}$$

$$Q_{rad} = \frac{1}{x^2}\left|\sum_{\ell=1}^{\infty}(2\ell + 1)(-1)^\ell(a_\ell + b_\ell)\right|^2 \tag{C-6}$$

Scattering Amplitudes

$$S_1(\theta) = \sum_{\ell=1}^{\infty} \frac{2\ell + 1}{\ell(\ell + 1)} [\, a_\ell \pi_\ell(\theta) + b_\ell \tau_\ell(\theta)] \tag{C-7}$$

$$S_2(\theta) = \sum_{\ell=1}^{\infty} \frac{2\ell + 1}{\ell(\ell + 1)} [\, b_\ell \pi_\ell(\theta) + a_\ell \tau_\ell(\theta)] \tag{C-8}$$

Intensity Factors

$$i_1(\theta) = | S_1(\theta) |^2 \tag{C-9}$$

$$i_2(\theta) = | S_2(\theta) |^2 \tag{C-10}$$

Recurrence formulas for Pi and Tau Functions

$$\pi_\ell(\theta) = \cos\theta \frac{(2\ell + 1)}{(\ell + 1)} \pi_{\ell-1}(\theta) - \frac{\ell}{\ell-1} \pi_{\ell-2}(\theta) \tag{C-11}$$

$$\tau_\ell(\theta) = \cos\theta [\, \pi_\ell(\theta) - \pi_{\ell-2}(\theta)] - (2\ell-1)\sin^2\theta \, \pi_{\ell-1}(\theta) + \pi_{\ell-2}(\theta) \tag{C-12}$$

Phase Function

$$p(\theta) = \frac{[\, i_1(\theta) + i_2(\theta)]}{2k^2 C_{sca}} \tag{C-13}$$

For all the above $\ell = 1,2,3,....$

DISTRIBUTION LIST FOR PUBLIC RELEASE

Commandant
U.S. Army Chemical School
ATTN: ATZN-CM-CC (S. Barnes)
Fort McClellan, AL 36205-5020

NASA/Marshall Space Flight Center
Deputy Director
Space Science Laboratory
Atmospheric Sciences Division
ATTN: E501 (Dr. George H. Fichtl)
Huntsville, AL 35802

NASA/Marshall Space Flight Center
Atmospheric Sciences Division
ATTN: Code ED-41
Huntsville, AL 35812

Deputy Commander
U.S. Army Strategic Defense Command
ATTN: CSSD-SL-L
Dr. Julius Q. Lilly
P.O. Box 1500
Huntsville, AL 35807-3801

Commander
U.S. Army Missile Command
ATTN: AMSMI-RD-AC-AD
Donald R. Peterson
Redstone Arsenal, AL 35898-5242

Commander
U.S. Army Missile Command
ATTN: AMSMI-RD-AS-SS
Huey F. Anderson
Redstone Arsenal, AL 35898-5253

Commander
U.S. Army Missile Command
ATTN: AMSMI-RD-AS-SS
B. Williams
Redstone Arsenal, AL 35898-5253

Commander
U.S. Army Missile Command
ATTN: AMSMI-RD-DE-SE
Gordon Lill, Jr.
Redstone Arsenal, AL 35898-5245

Commander
U.S. Army Missile Command
Redstone Scientific Information
Center
ATTN: AMSMI-RD-CS-R/Documents
Redstone, Arsenal, AL 35898-5241

Commander
U.S. Army Intelligence Center
and Fort Huachuca
ATTN: ATSI-CDC-C (Mr. Colanto)
Fort Huachuca, AZ 85613-7000

Northrup Corporation
Electronics Systems Division
ATTN: Dr. Richard D. Tooley
2301 West 120th Street, Box 5032
Hawthorne, CA 90251-5032

Commander - Code 3331
Naval Weapons Center
ATTN: Dr. Alexis Shlanta
China Lake, CA 93555

Commander
Pacific Missile Test Center
Geophysics Division
ATTN: Code 3250 (Terry E. Battalino)
Point Mugu, CA 93042-5000

Lockheed Missiles & Space Co., Inc.
Kenneth R. Hardy
Org/91-01 B/255
3251 Hanover Street
Palo Alto, CA 94304-1191

Commander
Naval Ocean Systems Center
ATTN: Code 54 (Dr. Juergen Richter)
San Diego, CA 92152-5000

Meteorologist in Charge
Kwajalein Missile Range
P.O. Box 67
APO San Francisco, CA 96555

U.S. Department of Commerce
Mountain Administration Support
Center
Library, R-51 Technical Reports
325 S. Broadway
Boulder, CO 80303

Dr. Hans J. Liebe
NTIA/ITS S 3
325 S. Broadway
Boulder, CO 80303

NCAR Library Serials
National Center for Atmos Rsch
P.O. Box 3000
Boulder, CO 80307-3000

HQDA
ATTN: DAMI-POI
Washington, DC 20310-1067

Mil Asst for Env Sci Ofc of
The Undersecretary of Defense
for Rsch & Engr/R&AT/E&LS
Pentagon - Room 3D129
Washington, DC 20301-3080

HQDA
DEAN-RMD/Dr. Gomez
Washington, DC 20314

Director
Division of Atmospheric Science
National Science Foundation
ATTN: Dr. Eugene W. Bierly
1800 G. Street, N.W.
Washington, DC 20550

Commander
Space & Naval Warfare System Command
ATTN: PMW-145-1G (LT Painter)
Washington, DC 20362-5100

Commandant
U.S. Army Infantry
ATTN: ATSH-CD-CS-OR
Dr. E. Dutoit
Fort Benning, GA 30905-5090

USAFETAC/DNE
Scott AFB, IL 62225

Air Weather Service
Technical Library - FL4414
Scott AFB, IL 62225-5458

USAFETAC/DNE
ATTN: Mr. Charles Glauber
Scott AFB, IL 62225-5008

Commander
U.S. Army Combined Arms Combat
ATTN: ATZL-CAW (LTC A. Kyle)
Fort Leavenworth, KS 66027-5300

Commander
U.S. Army Space Institute
ATTN: ATZI-SI (Maj Koepsell)
Fort Leavenworth, KS 66027-5300

Commander
U.S. Army Space Institute
ATTN: ATZL-SI-D
Fort Leavenworth, KS 66027-7300

Commander
Phillips Lab
ATTN: PL/LYP (Mr. Chisholm)
Hanscom AFB, MA 01731-5000

Director
Atmospheric Sciences Division
Geophysics Directorate
Phillips Lab
ATTN: Dr. Robert A. McClatchey
Hanscom AFB, MA 01731-5000

Raytheon Company
Dr. Charles M. Sonnenschein
Equipment Division
528 Boston Post Road
Sudbury, MA 01776
Mail Stop 1K9

Director
U.S. Army Materiel Systems
Analysis Activity
ATTN: AMXSY-MP (H. Cohen)
APG, MD 21005-5071

Commander
U.S. Army Chemical Rsch,
Dev & Engr Center
ATTN: SMCCR-OPA (Ronald Pennsyle)
APG, MD 21010-5423

Commander
U.S. Army Chemical Rsch,
Dev & Engr Center
ATTN: SMCCR-RS (Mr. Joseph Vervier)
APG, MD 21010-5423

Commander
U.S. Army Chemical Rsch,
Dev & Engr Center
ATTN: SMCCR-MUC (Mr. A. Van De Wal)
APG, MD 21010-5423

Director
U.S. Army Materiel Systems
Analysis Activity
ATTN: AMXSY-AT (Mr. Fred Campbell)
APG, MD 21005-5071

Director
U.S. Army Materiel Systems
Analysis Activity
ATTN: AMXSY-CR (Robert N. Marchetti)
APG, MD 21005-5071

Director
U.S. Army Materiel Systems
Analysis Activity
ATTN: AMXSY-CS (Mr. Brad W. Bradley)
APG, MD 21005-5071

Director
U.S. Army Research Laboratory
ATTN: AMSRL-D
2800 Powder Mill Road
Adelphi, MD 20783

Director
U.S. Army Research Laboratory
ATTN: AMSRL-OP-CI-A
(Technical Publishing)
2800 Powder Mill Road
Adelphi, MD 20783

Director
U.S. Army Research Laboratory
ATTN: AMSRL-OP-CI-AD, Record Copy
2800 Powder Mill Road
Adelphi, MD 20783

Director
U.S. Army Research Laboratory
ATTN: AMSRL-SS-SH
Dr. Z.G. Sztankay
2800 Powder Mill Road
Adelphi, MD 20783

National Security Agency
ATTN: W21 (Dr. Longbothum)
9800 Savage Road
Ft George G. Meade, MD 20755-6000

U. S. Army Space Technology
and Research Office
ATTN: Brenda Brathwaite
5321 Riggs Road
Gaithersburg, MD 20882

OIC-NAVSWC
Technical Library (Code E-232)
Silver Springs, MD 20903-5000

The Environmental Research
Institute of Michigan
ATTN: IRIA Library
P.O. Box 134001
Ann Arbor, MI 48113-4001

Commander
U.S. Army Research Office
ATTN: DRXRO-GS (Dr. W.A. Flood)
P.O. Box 12211
Research Triangle Park, NC 27709

Dr. Jerry Davis
North Carolina State University
Department of Marine, Earth, &
Atmospheric Sciences
P.O. Box 8208
Raleigh, NC 27650-8208

Commander
U. S. Army CECRL
ATTN: CECRL-RG (Dr. H. S. Boyne)
Hanover, NH 03755-1290

Commanding Officer
U.S. Army ARDEC
ATTN: SMCAR-IMI-I, Bldg 59
Dover, NJ 07806-5000

U.S. Army Communications-Electronics
Command EW/RSTA Directorate
ATTN: AMSEL-RD-EW-OP
Fort Monmouth, NJ 07703-5206

Commander
U.S. Army Satellite Comm Agency
ATTN: DRCPM-SC-3
Fort Monmouth, NJ 07703-5303

6585th TG (AFSC)
ATTN: RX (CPT Stein)
Holloman AFB, NM 88330

Department of the Air Force
OL/A 2nd Weather Squadron (MAC)
Holloman AFB, NM 88330-5000

PL/WE
Kirtland AFB, NM 87118-6008

Director
U.S. Army TRADOC Analysis Command
ATTN: ATRC-WSS-R
White Sands Missile Range, NM 88002

USAF Rome Laboratory Technical
Library, FL2810 Corridor W, Site 262,
RL//SUL (DOCUMENTS LIBRARY)
26 Electronics Parkway, Bldg 106
Griffiss AFB, NY 13441-4514

AFMC/DOW
Wright-Patterson AFB, OH 0334-5000

Commandant
U.S. Army Field Artillery School
ATTN: ATSF-TSM-TA
Mr. Charles Taylor
Fort Sill, OK 73503-5600

Commander
Naval Air Development Center
ATTN: Al Salik (Code 5012)
Warminister, PA 18974

Commander
U.S. Army Dugway Proving Ground
ATTN: STEDP-MT-DA-M
Mr. Paul Carlson
Dugway, UT 84022

Commander
U.S. Army Dugway Proving Ground
ATTN: STEDP-MT-DA-L
Dugway, UT 84022

Commander
U.S. Army Dugway Proving Ground
ATTN: STEDP-MT-M (Mr. Bowers)
Dugway, UT 84022-5000

Defense Technical Information Center
ATTN: DTIC-FDAC (2)
Cameron Station
Alexandria, VA 22314

Commanding Officer
U.S. Army Foreign Science &
Technology Center
ATTN: CM
220 7th Street, NE
Charlottesville, VA 22901-5396

Naval Surface Weapons Center
Code G63
Dahlgren, VA 22448-5000

Commander
U.S. Army OEC
ATTN: CSTE-EFS
Park Center IV
4501 Ford Ave
Alexandria, VA 22302-1458

Commander and Director
U.S. Army Corps of Engineers
Engineer Topographics Laboratory
ATTN: ETL-GS-LB
Fort Belvoir, VA 22060

TAC/DOWP
Langley AFB, VA 23665-5524

U.S. Army Topo Engineering Center
ATTN: CETEC-ZC
Fort Belvoir, VA 22060-5546

Commander
Logistics Center
ATTN: ATCL-CE
Fort Lee, VA 23801-6000

Commander
USATRADOC
ATTN: ATCD-FA
Fort Monroe, VA 23651-5170

Science and Technology
101 Research Drive
Hampton, VA 23666-1340

Commander
U.S. Army Nuclear & Cml Agency
ATTN: MONA-ZB Bldg 2073
Springfield, VA 22150-3198